Chapter 4

Laser in steady-state regime

The preceding chapter was a general introduction to the principle of operation of lasers. It aimed at explaining the basic features of laser oscillation with the minimum amount of mathematical formalism. In this chapter and the following, we will develop in more details the theory of lasers. Indeed, beyond their major interest in technology and scientific and industrial applications, lasers are fascinating objects for the physicist. The domain of lasers physics is a research field by itself, which is linked with quite remote fields of physics.

The reason behind such a variety of phenomena lies in the fact that the laser equations, on spite of their simplicity, are *nonlinear differential equations*. The study of laser dynamics is thus linked to the study of open dynamical systems, with connections to nonlinear dynamics and deterministic chaos. For example, we will in this chapter encounter stable and unstable steady-state solutions, and so-called bifurcations when the stability of these solutions changes when one tunes a control parameter. We will also see that the laser threshold can, to some extent, be considered as a phase transition, thus linking laser physics to statistical physics and thermodynamics. In the case of two modes, laser physics becomes even richer, since we will have several types of possible steady-state solutions, in which only one mode or two mode oscillate. Through the nonlinear behaviour of the laser active medium, we will see how mode competition can lead to several types of behaviors where either the two modes oscillate simultaneously or where the two modes exhibit bistability. In this latter case, an intriguing situation occurs where two stable solutions exist, and the laser "chooses" between these two solutions based on its preceding history. Thus, by tuning a control parameter, the laser can exhibit hysteresis cycles.

The first aim of the present chapter is thus to derive these nonlinear laser equations, based on results on light propagation in atomic media that we obtained in Chapter 2. Section 4.1 details the derivation of these equations, based on the simple Lamb's model for the two-level atom that was presented

in Chapter 2. We then show how these equations can be generalized to more realistic laser media. Section 4.2 is dedicated to the derivation of the single-frequency laser steady-state solutions and their stability domains. Section 4.3 introduces the very important concept of adiabatic elimination and of laser dynamical classes. Finally, Section 4.4 extends the discussion of the laser steady-state regime to the case of two modes competing for the gain.

This chapter is accompanied by three complements. Complement 4A presents a more general derivation of the laser equations based on the density matrix formalism, which was introduced in Complement 2C. It allows one to understand how laser theory can be built on somewhat more solid grounds than the simple derivation given in the chapter itself. Moreover, the so-called Maxwell-Bloch equations that are obtained in this context illustrate the role of atomic coherences in laser operation.

Complement 4B illustrates the fact that lasers are nonlinear dynamical systems by studying an interesting phenomenon: injection locking. Indeed, similarly to Huygens' clocks or to any oscillators, two lasers can synchronize their oscillation frequencies when they are coupled. Beyond its fundamental interest, this phenomenon has important applications when it comes to transferring the spectral purity of a small power laser, with a well controlled frequency, to a more powerful one, or in some rotation sensors like the ring laser gyroscope. Moreover, it paves the way to laser mode-locking that will be studied in Chapter 5.

Finally, Complement 4C is devoted to descriptions of some important applications of laser energy in various domains, showing how the ability to be concentrated is the key to many applications of laser light.

4.1 Derivation of the single-frequency laser equations

In this section, we establish the equations of evolution of a single-frequency laser. We start by deriving the equation of evolution of the field. We then write the equation of evolution of the population inversion in three different cases: i) the two-level atom model of Chapter 2; ii) the three-level model; iii) the four-level model. A more general derivation, based on the formalism of the density operator for the atoms and on Maxwell-Bloch equations, is presented in Complement 4A.

4.1.1 Equation of evolution of the field

We consider a ring cavity as sketched in Figure 4.1. We assume that the active medium is spatially homogeneous and has a length L_a. We suppose that the laser field propagates in one direction only (the clockwise direction in Figure 4.1) and is monochromatic of frequency ω. We call z the abscissa

along the light propagation axis inside the cavity, with origin O, and we suppose that the intra-cavity field can be treated as a truncated plane wave ("top-hat beam") of transverse section area S, namely:

$$E(z,t) = \mathcal{A}(z,t)\,\mathrm{e}^{-\mathrm{i}(\omega t - kz)} + \text{c.c.} = 2\,\mathrm{Re}\Big[\mathcal{A}(z,t)\,\mathrm{e}^{-\mathrm{i}(\omega t - kz)}\Big]\,, \tag{4.1}$$

where we have supposed that the polarization of the intra-cavity field is fixed, allowing us to treat light as a scalar quantity. For example, in a cavity such as the one of Figure 4.1, the light polarization can be linear and orthogonal to the plane of the cavity. Moreover, in this section, we neglect the dispersion of the active medium and take the real part of k to be $k' = \omega/c$. $\mathcal{A}$ is called the slowly varying field complex amplitude, meaning that it depends on t and z in a much slower way than the phase term $\mathrm{e}^{-\mathrm{i}(\omega t - kz)}$, i.e.

$$\left|\frac{\partial}{\partial t}\mathcal{A}(t,z)\right| \ll \omega|\mathcal{A}(t,z)|\,, \tag{4.2}$$

$$\left|\frac{\partial}{\partial z}\mathcal{A}(t,z)\right| \ll |k|\;|\mathcal{A}(t,z)|\,. \tag{4.3}$$

The *slowly varying amplitude approximation* of Equations (4.2) and (4.3) means that the temporal variation of the amplitude over one time period $2\pi/\omega$ and the spatial variation of the amplitude over one wavelength are small. This approximation is usually fulfilled, except for lasers emitting pulses with a duration of a few femtoseconds. In the following, we make a stronger hypothesis. We indeed suppose that the laser operates in continuous regime or emits pulses which are much longer than the cavity round-trip time L_{cav}/c, where L_{cav} is the optical length of one round-trip inside the cavity. We moreover assume that the losses and gain per round-trip are small. This ensures that the mode intensity is almost the same everywhere inside the cavity.

At time t, let us consider the intra-cavity field $\mathcal{A}(z=0,t)$ at origin point O (see Figure 4.1). After one round-trip inside the cavity, i.e. after a delay L_{cav}/c, the field at point A is

$$\mathcal{A}\left(z=0, t+\frac{L_{\text{cav}}}{c}\right) = \sqrt{R_1R_2R_3(1-\alpha)}\,\mathcal{A}(z=0,t)\,\mathrm{e}^{\mathrm{i}k'L_{\text{cav}}}\,\mathrm{e}^{gL_{\text{a}}/2}\,, \tag{4.4}$$

where the coefficients R_i are the intensity reflection coefficients of the mirrors and where α holds for the other cavity losses (scattering, residual absorption, diffraction losses,...). g is the intensity gain coefficient of the active medium.

Since $k' = \omega/c$, the factor $\exp(ik'L_{\text{cav}})$ is equal to 1 as soon as the laser frequency is equal to one of the cavity eigenfrequencies ω_q:

$$\omega_q = q\,2\pi\frac{c}{L_{\text{cav}}} = q\,\Omega_{\text{cav}}\,, \tag{4.5}$$

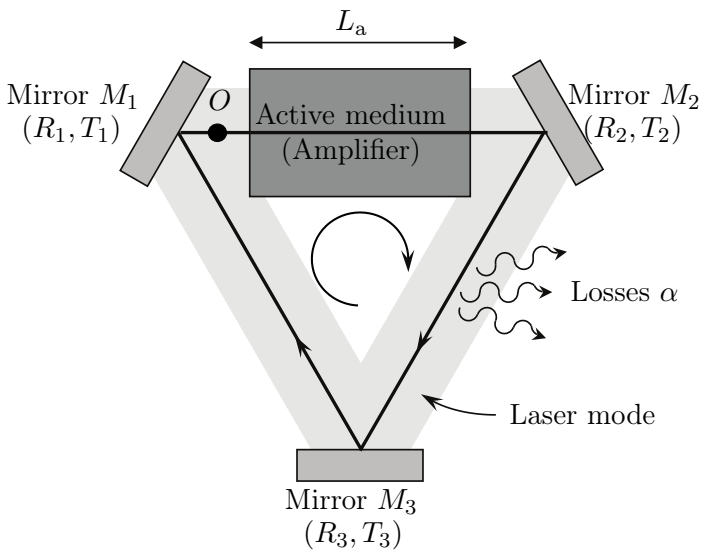

Figure 4.1: Unidirectional ring laser. O is the origin point for the abscissa z.

where q is an integer. We thus retrieve the longitudinal modes and the free spectral range $\Omega_{\rm cav}$ defined in Section 3.3.1.

Since we suppose that the laser operates in continuous regime, or emits pulses whose duration is much longer than $L_{\rm cav}/c$, we can focus on the value of the field amplitude at the origin $z = 0$. We thus skip the space dependence of $\mathcal{A}(z,t)$ and write:

$$\mathcal{A}(t) = \mathcal{A}(z=0,t) \; . \tag{4.6}$$

Moreover, since we suppose that the losses and gain per round-trip are small, we can perform a first-order Taylor expansion of the left-hand side of equation (4.4):

$$\mathcal{A}\left(t + \frac{L_{\rm cav}}{c}\right) \simeq \mathcal{A}(t) + \frac{L_{\rm cav}}{c}\,\frac{{\rm d}\mathcal{A}}{{\rm d}t} \; . \tag{4.7}$$

Then, using the expansion

$$\exp\left(\frac{gL_{\rm a}}{2}\right) \simeq 1 + \frac{gL_{\rm a}}{2} \; , \tag{4.8}$$

we obtain the following first-order differential equation for the field amplitude:

$$\frac{{\rm d}\mathcal{A}}{{\rm d}t} = -\frac{1}{2\tau_{\rm cav}}\mathcal{A} + \frac{cg}{2}\frac{L_{\rm a}}{L_{\rm cav}}\mathcal{A} \; , \tag{4.9}$$

with

$$\tau_{\rm cav} = \frac{L_{\rm cav}}{2c}\left[1 - \sqrt{R_1R_2R_3(1-\alpha)}\right]^{-1} \; . \tag{4.10}$$

Let us now use the definition of the laser cross section σ_{L} that relates the gain to the population inversion density $\Delta n = n_b - n_a$ in the active medium (see Equation 2.123):

$$g = \sigma_{\mathrm{L}}\, \Delta n \; . \tag{4.11}$$

Equation (4.9) then becomes:

$$\frac{\mathrm{d}\mathcal{A}}{\mathrm{d}t} = -\frac{\mathcal{A}}{2\tau_{\mathrm{cav}}} + c\frac{\sigma_{\mathrm{L}}}{2}\frac{L_{\mathrm{a}}}{L_{\mathrm{cav}}}\,\Delta n\,\mathcal{A} \; . \tag{4.12}$$

The quantity τ_{cav} defined by Equation 4.10 is called the *lifetime of the photons inside the cavity*. Indeed, in the absence of gain (the so-called "cold cavity"), Equation (4.12) shows that the intracavity field amplitude decays exponentially, i. e., $\mathcal{A}(t) = \mathcal{A}(0)\,\mathrm{e}^{-t/2\tau_{\mathrm{cav}}}$. The intensity, proportional to $|\mathcal{A}|^2$, thus decays with a lifetime τ_{cav}. Its inverse is the decay rate γ_{cav} of the intracavity intensity:

$$\gamma_{\mathrm{cav}} = \frac{1}{\tau_{\mathrm{cav}}} \; . \tag{4.13}$$

Since the losses are supposed to be small $[1 - R_1R_2R_3(1-\alpha) \ll 1]$, we obtain

$$\tau_{\mathrm{cav}} = \frac{L_{\mathrm{cav}}/c}{\Upsilon} \; , \tag{4.14}$$

where we have introduced the *total losses* per cavity round-trip:

$$\Upsilon = (1-R_1) + (1-R_2) + (1-R_3) + \alpha \; . \tag{4.15}$$

The physical meaning of τ_{cav} appears clearly in Equation (4.14): τ_{cav} is the duration of one round-trip divided by the losses per round-trip inside the cavity. It is also sometimes useful to define the quality factor Q_{cav} of the cavity (see Complement 3A):

$$Q_{\mathrm{cav}} = \omega\,\tau_{\mathrm{cav}} \; . \tag{4.16}$$

To gain some physical insight in the laser physics, it is worth transforming Equation (4.12), which governs the evolution of the complex amplitude $\mathcal{A}$, into an equation governing the number of photons $\mathcal{N}$ stored inside the cavity[1].

Since we have supposed that the intra-cavity beam is a truncated plane wave of cross section are S, its Poynting vector, i. e., its directional energy flux density, is oriented along z with a modulus given by Equation (2.54):

$$\Pi = 2\varepsilon_0\, c|\mathcal{A}|^2 \; . \tag{4.17}$$

[1]It should be noted that the word "photon" is used here only as a natural unit of energyy. A rigorous definition of the photon requires the field quantization, as shown in PHY562.

The photon flux inside the cavity is thus $\Pi S/\hbar\omega$. Since the round-trip time is given by $L_{\rm cav}/c$, we can define the number of photons inside the cavity:

$$\mathcal{N} = \frac{\Pi S}{\hbar\omega}\frac{L_{\rm cav}}{c} = \frac{\Pi\, V_{\rm cav}}{\hbar\omega c} \ , \tag{4.18}$$

where we have introduced the volume occupied by the top-hat mode inside the cavity:

$$V_{\rm cav} = S\, L_{\rm cav} \ . \tag{4.19}$$

Using Equations (4.17) and (4.19), we obtain:

$$\mathcal{N} = \frac{2\varepsilon_0\, L_{\rm cav}}{\hbar\omega} S|\mathcal{A}|^2 \ . \tag{4.20}$$

Equation (4.12) then rewrites

$$\frac{{\rm d}\mathcal{N}}{{\rm d}t} = -\frac{\mathcal{N}}{\tau_{\rm cav}} + \kappa\, \Delta N\, \mathcal{N} \ , \tag{4.21}$$

where we have introduced the population inversion ΔN:

$$\Delta N = N_b - N_a = V_{\rm a}\, \Delta n = V_{\rm a}(n_b - n_a) \ . \tag{4.22}$$

$V_{\rm a}$ is the volume occupied by the laser mode in the active medium of length $L_{\rm a}$:

$$V_{\rm a} = S\, L_{\rm a} \ . \tag{4.23}$$

Finally, the atom-photon coupling coefficient κ in Equation (4.21) is given by:

$$\kappa = \frac{c\,\sigma_{\rm L}}{V_{\rm cav}} \ . \tag{4.24}$$

4.1.2 Equation of evolution of the population inversion

Equation (4.21) has two terms: the loss term and the gain term. This latter term contains the population inversion ΔN. A full description of the laser behaviour thus requires the derivation of an evolution equation for ΔN, which we obtain below following three different models. A more general derivation based on so-called Bloch equations will be given in Complement 4A.

a. Rate equation for Lamb's model

Let us recall that the Lamb's model consists in assuming that the two levels a and b of the laser transition have the same lifetimes $1/\Gamma_{\rm D}$ (see Figure 4.2). Taking then the difference between Equations (2.38) and (2.39), we obtain:

$$\frac{\rm d}{{\rm d}t}\Delta N = \Lambda_b - \Lambda_a - \Gamma_{\rm D}\Delta N - \Gamma_{\rm D}\, s\, \Delta N \ . \tag{4.25}$$

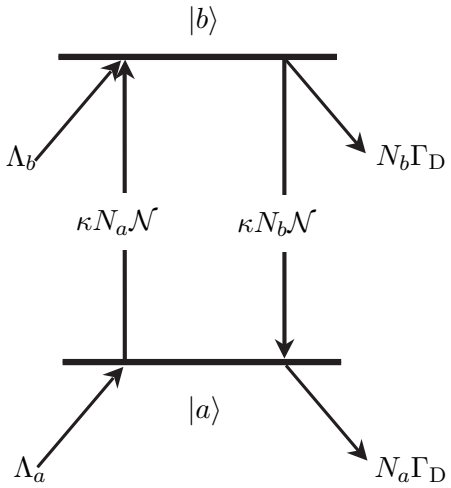

Figure 4.2: Transition rates in Lamb's model.

If $|\omega - \omega_0| \ll \Gamma_D$, the saturation parameter s is related to the number of photons $\mathcal{N}$ by (see Equations 2.23, 2.54, 2.59, 2.114, and 4.18):

$$s \simeq \frac{I}{I_{sat}} = 2\frac{\kappa}{\Gamma_D}\mathcal{N} \, . \tag{4.26}$$

The pumping term $\Lambda_b - \Lambda_a$ in Equation (4.25) can be cast in the following form:

$$\Lambda_b - \Lambda_a = \Gamma_D \, \Delta N_0 \, , \tag{4.27}$$

by introducing the dimensionless pumping parameter ΔN_0. Equation (4.25) then becomes:

$$\frac{d\Delta N}{dt} = \Gamma_D(\Delta N_0 - \Delta N) - 2\kappa\Delta N\mathcal{N} \, . \tag{4.28}$$

The meanings of the three terms on the right-hand side of Equation (4.28) are clear. The first one, $\Gamma_D\Delta N_0$, corresponds to pumping. $\Gamma_D\Delta N$ describes the relaxation of the population inversion, and $\tau_D = 1/\Gamma_D$ will from now on be called *the lifetime of the population inversion*. The term $-2\kappa\Delta N\mathcal{N}$ corresponds to stimulated emission and absorption. It is the symmetric of the term $+\kappa\Delta N\mathcal{N}$ in Equation (4.21). The coefficient -2 is related to the fact that, in Lamb's model, each time one photon is emitted ($\mathcal{N} \rightarrow \mathcal{N} + 1$), the population inversion decreases by two units ($\Delta N \rightarrow \Delta N - 2$) because level $|b\rangle$ loses one atom while level $|a\rangle$ gains it.

b. Rate equations for the three-level system

Let us next consider the three-level system, which we have already described in Section 3.5. The peculiarity of such a system is that the laser transition

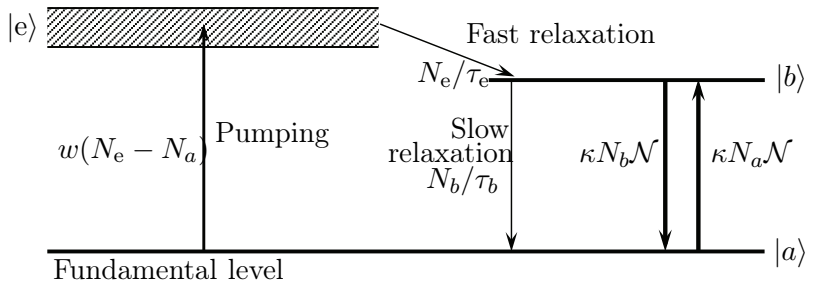

Figure 4.3: Three-level system.

ends on the ground state, as shown in Figure 4.3. The rate equations for such atoms are obtained by adding the stimulated emission and absorption terms to Equations (3.31, 3.32), leading to

$$\frac{\mathrm{d}N_\mathrm{e}}{\mathrm{d}t} = w(N_a - N_\mathrm{e}) - \frac{N_\mathrm{e}}{\tau_\mathrm{e}} \,, \tag{4.29}$$

$$\frac{\mathrm{d}N_b}{\mathrm{d}t} = \frac{N_\mathrm{e}}{\tau_\mathrm{e}} - \frac{N_b}{\tau_b} - \kappa(N_b - N_a)\mathcal{N} \,, \tag{4.30}$$

$$\frac{\mathrm{d}N_a}{\mathrm{d}t} = -w(N_a - N_\mathrm{e}) + \frac{N_b}{\tau_b} + \kappa(N_b - N_a)\mathcal{N} \,. \tag{4.31}$$

Suppose that the system satisfies the same conditions as in Section 3.5, i. e., $\tau_\mathrm{e} \ll \tau_b$ and $w\tau_\mathrm{e} \ll 1$. Then, level $|\mathrm{e}\rangle$ decays quasi instantaneously to level $|b\rangle$, and we can consider that $N_\mathrm{e} \simeq 0$. Then, by taking the difference between Equations (4.30) and (4.31), and remembering that the total number of atoms $N = N_a + N_b$ remains constant, we are left with:

$$\frac{\mathrm{d}}{\mathrm{d}t}\Delta N = \Gamma(\Delta N_0 - \Delta N) - 2\kappa\Delta N\mathcal{N} \,, \tag{4.32}$$

where

$$\Gamma = w + \frac{1}{\tau_b} \,, \tag{4.33}$$

$$\Delta N_0 = N\frac{w\tau_b - 1}{w\tau_b + 1} \,. \tag{4.34}$$

We notice that the factor of 2 in front of the stimulated emission term is also present here, due to the infinite lifetime of the lower level of the laser transition.

c. Rate equations for the four-level system

We have already written the rate equations of the four-level system of Figure 4.4 in the absence of laser light (see Section 3.6). Guided by the results

derived in the framework of Lamb's model, we add the terms corresponding to absorption and stimulated emission inside the laser to Equations (3.38–3.41). We obtain:

$$\frac{\mathrm{d}N_\mathrm{e}}{\mathrm{d}t} = w(N_\mathrm{g} - N_\mathrm{e}) - \frac{N_\mathrm{e}}{\tau_\mathrm{e}} \,, \tag{4.35}$$

$$\frac{\mathrm{d}N_b}{\mathrm{d}t} = \frac{N_\mathrm{e}}{\tau_\mathrm{e}} - \frac{N_b}{\tau_b} - \kappa(N_b - N_a)\mathcal{N} \,, \tag{4.36}$$

$$\frac{\mathrm{d}N_a}{\mathrm{d}t} = \frac{N_b}{\tau_b} - \frac{N_a}{\tau_a} + \kappa(N_b - N_a)\mathcal{N} \,, \tag{4.37}$$

$$\frac{\mathrm{d}N_\mathrm{g}}{\mathrm{d}t} = \frac{N_\mathrm{e}}{\tau_a} - w(N_\mathrm{g} - N_\mathrm{e}) \,. \tag{4.38}$$

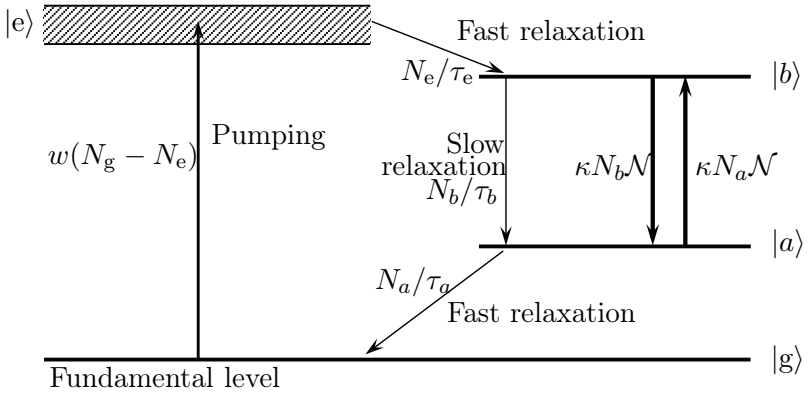

Figure 4.4: Four-level system.

If this four-level system is ideal, as we have seen in Section 3.6, the lifetimes of levels $|\mathrm{e}\rangle$ and $|a\rangle$ are so short ($\tau_\mathrm{e}, \tau_a \ll \tau_b$ and $w\tau_\mathrm{e} \ll 1$) that we can neglect their populations: $N_a \simeq 0$ and $N_\mathrm{e} \simeq 0$. Then $\Delta N = N_b$ and Equations (4.35–4.38) simply become:

$$\frac{\mathrm{d}\Delta N}{\mathrm{d}t} = w\, N_\mathrm{g} - \frac{\Delta N}{\tau_b} - \kappa \Delta N \mathcal{N} \,. \tag{4.39}$$

Using the fact that $N_\mathrm{g} + N_b = N$, Equation (4.39) can be re-written:

$$\frac{\mathrm{d}\Delta N}{\mathrm{d}t} = \Gamma(\Delta N_0 - \Delta N) - \kappa \Delta N \mathcal{N} \,, \tag{4.40}$$

where

$$\Gamma = w + \frac{1}{\tau_b} \,, \tag{4.41}$$

$$\Delta N_0 = N \frac{w\tau_b}{1 + w\tau_b} \,. \tag{4.42}$$

Comparing Equation (4.40) with Equations (4.28) and (4.32), we notice that there is no longer a factor of 2 in front of the term $\kappa\Delta N\mathcal{N}$ responsible for stimulated emission. This is due to the fact that thanks to the fast decay of level $|a\rangle$, each photon emission leads to a decrease of ΔN by one unit only.

d. Generalization

By comparing Equations (4.28), (4.32), and (4.40), we see that the rate equation for the population inversion keeps the same form, except for a numerical factor in front of the term describing light-atom interaction (the saturation term). Following Siegman[2], we thus write the general laser rate equations in the following manner:

$$\frac{\mathrm{d}\mathcal{N}}{\mathrm{d}t} = -\frac{\mathcal{N}}{\tau_{\mathrm{cav}}} + \kappa\Delta N\mathcal{N}\,, \tag{4.43}$$

$$\frac{\mathrm{d}\Delta N}{\mathrm{d}t} = \Gamma(\Delta N_0 - \Delta N) - 2^*\,\kappa\Delta N\mathcal{N}\,, \tag{4.44}$$

where the coefficient 2^* is equal to 1 for a four-level system, 2 for a three-level system, and can take other values for more complicated level structures. Moreover, one should notice that the term ΔN_0 depends on the details of the considered laser. In particular, it is not always proportional to the power injected in the pumping process. For example, by simply comparing Equations (4.42) and (4.34), one can see that ΔN_0 is always positive for a four-level system while it can vary between $-N$ and $+N$ for a three-level system, as already shown in Figure 3.18. Finally, in the following, we will alternatively use Γ or its inverse τ, the lifetime of the population inversion:

$$\tau = \frac{1}{\Gamma}\,. \tag{4.45}$$

We also notice from (4.43) that $\mathrm{d}\mathcal{N}/\mathrm{d}t = 0$ if $\mathcal{N} = 0$: the laser cannot start by itself from 0. In order to start, a laser needs spontaneous emission, which will be introduced in a phenomenological way in Sections 4.2.4b and 5.4 and in a more rigorous manner in PHY562.

4.2 Single-frequency laser in steady-state regime

In this section we derive the steady-state solutions for the single-frequency laser Equations (4.43) and (4.44), and we discuss their stability and the associated laser frequency and phase. The use of Equations (4.43) and (4.44) will allow us to be more rigorous than in Section 3.1 and to go far beyond.

[2] A.E. Siegman, *Lasers*, University Science Books, (1986).

4.2.1 Steady-state solutions

a. Determination of the steady-state solutions for $\mathcal{N}$ and ΔN

Let us look for the steady-state solutions of Equations (4.43) and (4.44) by taking $\frac{\mathrm{d}\mathcal{N}}{\mathrm{d}t} = 0$ and $\frac{\mathrm{d}\Delta N}{\mathrm{d}t} = 0$. This leads to:

$$\mathcal{N}\left(\kappa\Delta N - \frac{1}{\tau_{\mathrm{cav}}}\right) = 0 \ , \tag{4.46}$$

$$\Gamma\Delta N_0 = \Gamma\Delta N + 2^*\,\kappa\Delta N\mathcal{N} \ . \tag{4.47}$$

In order to find the solutions, Equations (4.46) and (4.47) must be solved simultaneously. We first notice that Equation (4.46) has two possible solutions:

$$\text{i) } \mathcal{N} = 0 \ , \tag{4.48}$$

or

$$\text{ii) } \kappa\Delta N - \frac{1}{\tau_{\mathrm{cav}}} = 0 \ . \tag{4.49}$$

In the following, we successively study these two solutions.

i) "OFF" *solution*:

The first solution, obtained from Equation (4.48) corresponds to the absence of photons inside the cavity. We will thus label it as the "OFF" solution. By inserting $\mathcal{N} = 0$ into Equation (4.47), we obtain the value of ΔN corresponding to this solution. This finally leads to:

$$\Delta N_{\mathrm{OFF}} = \Delta N_0 \ , \tag{4.50}$$

$$\mathcal{N}_{\mathrm{OFF}} = 0 \ . \tag{4.51}$$

It corresponds to the laser turned off. There is no light inside the cavity and the population inversion is not saturated.

ii) "ON" *solution*:

The second solution corresponds to Equation (4.49), that leads to the following value for ΔN:

$$\Delta N_{\mathrm{ON}} = \frac{1}{\kappa\tau_{\mathrm{cav}}} = \frac{S\Upsilon}{\sigma} = \Delta N_{\mathrm{th}} \ , \tag{4.52}$$

where, as defined in Equation (4.15), Υ are the total losses per round-trip. By injecting this value of ΔN into Equation (4.47), one obtains the following value for $\mathcal{N}$:

$$\mathcal{N}_{\mathrm{ON}} = \frac{1}{2^*\kappa\tau}\left(\frac{\Delta N_0}{\Delta N_{\mathrm{th}}} - 1\right) = \frac{1}{2^*\kappa\tau}(r-1) = \mathcal{N}_{\mathrm{sat}}(r-1) \ , \tag{4.53}$$

with

$$\mathcal{N}_{\rm sat} = \frac{1}{2^*\kappa\tau} \ , \tag{4.54}$$

and where the *relative excitation* r has been defined according to

$$r = \frac{\Delta N_0}{\Delta N_{\rm th}} \ . \tag{4.55}$$

Since the number of photons can only be positive, we consider this solution when $r > 1$ only. We labeled it "ON" because, as seen from Equation (4.53), it corresponds to a number of photons larger than 0 when $r > 1$. Using Equation (4.26), Equation (4.53) becomes:

$$I_{\rm ON} = I_{\rm sat}(r-1) \ . \tag{4.56}$$

This solution corresponds to the laser turned on. It is worth noticing from Equation (4.52) that the value of the population inversion remains clamped to its value at threshold $\Delta N_{\rm th}$ for any value of the pumping, i.e. of the unsaturated population inversion ΔN_0, as already noticed in Figure 3.3. This is easily understood by rewriting Equations (4.55) and (4.56) in the following manner:

$$\Delta N_{\rm th} = \frac{\Delta N_0}{1 + I/I_{\rm sat}} \ . \tag{4.57}$$

One can thus see that once the laser is on, the population inversion gets saturated by the intra-cavity intensity and remains blocked to the value $\Delta N_{\rm th}$. If there were no such saturation, the round-trip gain would remain larger than the losses, leading to an unlimited exponential increase of the intensity. It is thus the nonlinear saturation which is responsible for the stabilisation of the laser intensity.

b. Stability of the steady-state solutions

We can see that there exists two steady-state solutions, the so-called "ON" and "OFF" solutions, which coexist for $\Delta N_0 > \Delta N_{\rm th}$. In the following, we analyze their stability to know which solution will be chosen by the laser.

• *Stability of the* "OFF" *solution*

Let us suppose that we move the laser slightly away from the "OFF" solution:

$$\Delta N(t) = \Delta N_{\rm OFF} + x(t) = \Delta N_0 + x(t) \ , \tag{4.58}$$

$$\mathcal{N}(t) = \mathcal{N}_{\rm OFF} + y(t) = y(t) \ , \tag{4.59}$$

where $x(t)$ et $y(t)$ are small quantities. By injecting (4.58) and (4.59) into the Equations (4.43) and (4.44) for the evolution of the laser, and keeping only

first-order terms in x and y one gets the *linearized equations of evolution*:

$$\dot{x}(t) = -\frac{x(t)}{\tau} - 2^* \kappa \Delta N_0 \, y(t) \; , \tag{4.60}$$

$$\dot{y}(t) = \left(\kappa \Delta N_0 - \frac{1}{\tau_{\rm cav}} \right) y(t) \; , \tag{4.61}$$

which can be rewritten:

$$\begin{pmatrix} \dot{x} \\ \dot{y} \end{pmatrix} = M \begin{pmatrix} x \\ y \end{pmatrix} \; . \tag{4.62}$$

The matrix M is given by

$$\begin{pmatrix} -1/\tau & -2^* \kappa \Delta N_0 \\ 0 & \kappa \Delta N_0 - 1/\tau_{\rm cav} \end{pmatrix} \; . \tag{4.63}$$

The eigenvalues of M are $\lambda_1 = -1/\tau$ and $\lambda_2 = \kappa \Delta N_0 - 1/\tau_{\rm cav}$. Consequently, the general solution of Equation (4.63) takes the form:

$$x(t) = x_1 \mathrm{e}^{\lambda_1 t} + x_2 \mathrm{e}^{\lambda_2 t} \; , \tag{4.64}$$

$$y(t) = y_1 \mathrm{e}^{\lambda_1 t} + y_2 \mathrm{e}^{\lambda_2 t} \; , \tag{4.65}$$

where x_1, x_2, y_1, y_2 depend on the initial conditions. The solution "OFF" will consequently be stable if $x(t)$ and $y(t)$ come back to zero. This requires that the real parts of these two eigenvalues λ_1 and λ_2, called Lyapunov exponents, are both negative, i.e. that $\Delta N_0 < 1/\kappa \tau_{\rm cav} = \Delta N_{\rm th}$. The laser is then said to be *below threshold*. The gain term $\kappa F \Delta N$ is smaller than the losses $-F/\tau_{\rm cav}$ in the equation of evolution (4.43) of the intensity. Above threshold, the solution "OFF" is no longer stable.

In summary (see Table 4.1), the laser threshold is characterized by an unsaturated population inversion $\Delta N_0 = \Delta N_{\rm th}$ given by

$$\Delta N_{\rm th} = \frac{1}{\kappa \tau_{\rm cav}} \; , \tag{4.66}$$

and by the fact that the unsaturated gain is exactly equal to the losses, as can be seen using (4.52) to calculate the gain at threshold:

$$g_{\rm th} L_{\rm a} = \sigma_{\rm L} \Delta n_{\rm th} L_{\rm a} = \sigma_{\rm L} \frac{\Delta N_{\rm th}}{L_{\rm a} S} L_{\rm a} = \Upsilon \; . \tag{4.67}$$

It is worth noticing also that, at threshold, the Lyapunov exponent λ_2 is equal to zero. Thus, the system takes an infinite time to reach its steady-state. This critical slowing-down is characteristic of a system at a phase transition, an analogy that will be developed in Section 4.2.3.

• *Stability of the* "ON" *solution*

	ΔN_0	Unsaturated gain	ΔN	Saturated gain
Below threshold	$\Delta N_0 < \Delta N_{\rm th}$	$<$ Losses	$\Delta N = \Delta N_0$	
At threshold	$\Delta N_0 = \Delta N_{\rm th}$	$=$ Losses	$\Delta N = \Delta N_0 = \Delta N_{\rm th}$	
Above threshold	$\Delta N_0 > \Delta N_{\rm th}$	$>$ Losses	$\Delta N = \Delta N_{\rm th}$	$=$ Losses

Table 4.1: Characteristics of a laser below, at, and above threshold

Once the laser oscillates, Equation (4.57) becomes valid. It shows, as summarized in Table 4.1, that when the laser is on, the saturated population inversion is

$$\Delta N = \Delta N_{\rm th} = \frac{1}{\kappa \tau_{\rm cav}} \,, \tag{4.68}$$

showing that the saturated gain is equal to the losses. This condition ensures the equality of the gain and losses terms in Equation (4.43): the laser is in steady-state regime because the saturated gain exactly compensates for the losses at every round-trip inside the cavity.

To make sure that this solution is stable above threshold, let us move the laser slightly away from the "ON" solution:

$$\Delta N(t) = \Delta N_{\rm ON} + x(t) = \Delta N_{\rm th} + x(t) \,, \tag{4.69}$$

$$\mathcal{N}(t) = \mathcal{N}_{\rm ON} + y(t) \,, \tag{4.70}$$

where $x(t)$ and $y(t)$ are supposed to be small. By injecting (4.69) and (4.70) in Equations (4.43) and (4.44) and keeping only first-order terms, one gets an equation similar to (4.62) where the matrix M is given by

$$M = \begin{pmatrix} -r/\tau & -2^*/\tau_{\rm cav} \\ (r-1)/2^*\tau & 0 \end{pmatrix} \,. \tag{4.71}$$

The eigenvalues of this matrix are:

$$\lambda_\pm = -\frac{r}{2\tau} \pm \frac{1}{2}\sqrt{\left(\frac{r}{\tau}\right)^2 - \frac{4(r-1)}{\tau\,\tau_{\rm cav}}} \,. \tag{4.72}$$

One can see that for $r > 1$, the real parts of the two eigenvalues are always negative, confirming the stability of the "ON" solution.

c. Comparison between three- and four-level systems

Figure 4.5 summarizes the preceding discussion about the steady-state solutions of the laser and permits to confirm the behavior that we had anticipated in Figure 3.3. In particular, it shows that the threshold actually corresponds to the transition from one steady-state solution to the other occurring when

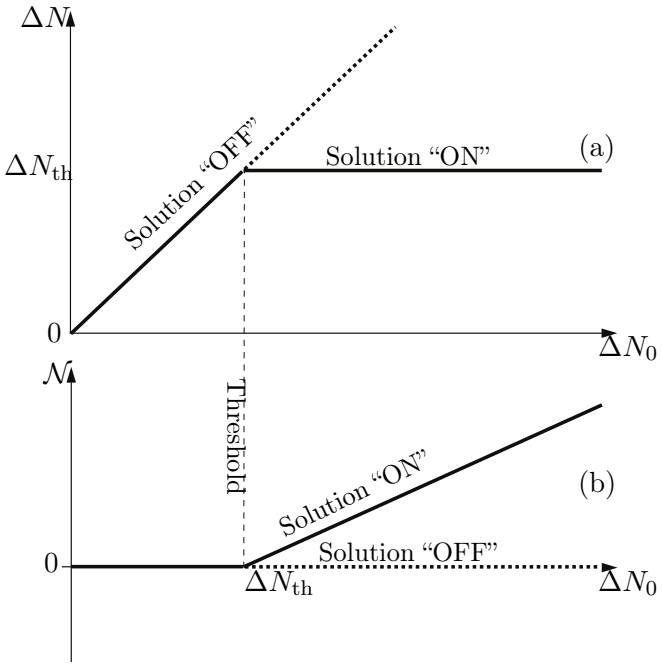

Figure 4.5: Steady-state solutions of the laser versus unsaturated population inversion. Full line: stable solution; dotted line: unstable solution.

the unsaturated gain exceeds the losses. This sudden change in stability of a give solution is named a *bifurcation* in the context of dynamical systems. It is plotted versus the unsaturated population inversion ΔN_0. As seen earlier, ΔN_0 does not evolve versus the pumping rate w in the same manner in a three-level and in a four-level system (see Sections 3.5 and 3.6). If we imagine that we can find a three-level system and a four-level system exhibiting identical parameters, Figure 4.6 compares their behaviours as functions of w. One can see that the three-level system presents two disadvantages[3]: i) an important amount of pumping is used to bleach the medium before gain can be obtained and ii) since I_{sat} is twice smaller for a three-level system than for a four-level system, the slope of the evolution of the power versus pumping is also twice smaller.

d. Output power: optimal output coupling

The steady-state solutions of the laser Equations (4.43) and (4.44) allow us to determine the number of photons and consequently the *intensity* inside

[3]One should not forget, however, that the first laser, namely the ruby laser [T.H. Maiman, *Stimulated Optical Radiation in Ruby*, Nature 187, 493 (1960)], was based on a three-level system. In the same vein, the Erbium doped amplifying fiber, a major component of optical fibers telecommunication system, uses a three-level system (cf. section 3.5.2).

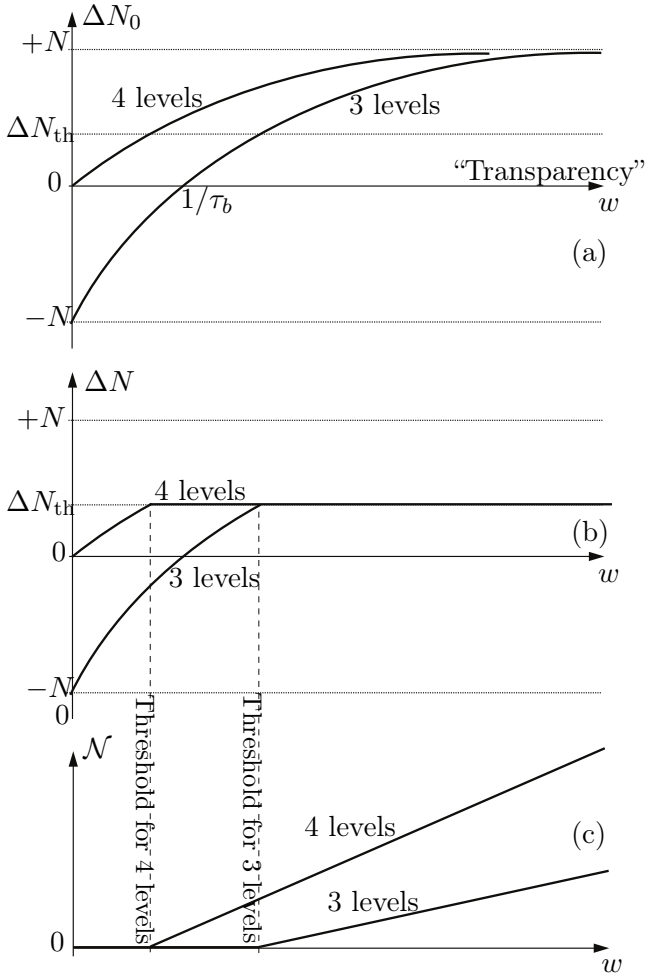

Figure 4.6: Compared evolutions versus pumping rate w of (a) the unsaturated population inversion ΔN_0, (b) the population inversion ΔN and (c) the number of photons $\mathcal{N}$ for a three-level and a four-level system.

the laser cavity. For example, for the laser of Figure 4.7 that has one output coupling mirror of transmission T and where we call all the other losses (imperfect reflection from other mirrors, scattering, absorption,...) α, the total losses per round-trip are $\Upsilon = T + \alpha$ and, according to Equation (4.56), the intra-cavity intensity is

$$I = I_{\rm sat}(r-1) = I_{\rm sat}\left(\frac{g_0 L_{\rm a}}{T+\alpha} - 1\right) , \tag{4.73}$$

where $L_{\rm a}$ is the length of the active medium. As expected, for a given value of the gain g_0, the smaller the mirror transmission T (and thus the losses), the larger the *intracavity intensity*.

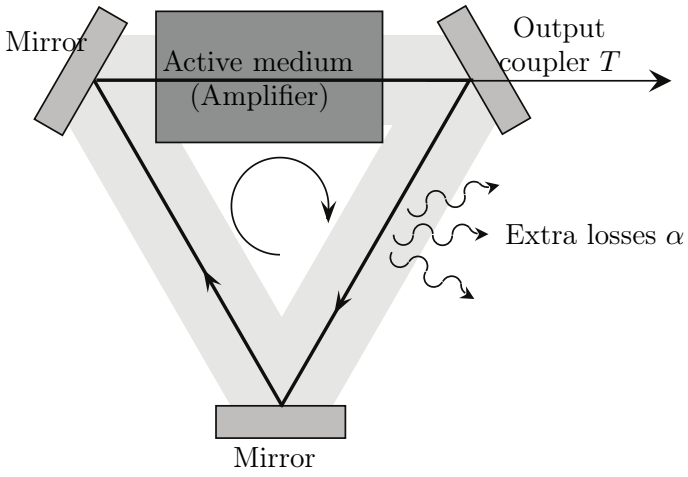

Figure 4.7: Laser with an output coupling mirror with transmission T.

One should not deduce from this argument that the laser *output intensity* is optimized by minimizing T. Indeed, the laser output intensity is given by:

$$I_{\rm out} = T\, I_{\rm sat} \left(\frac{g_0 L_{\rm a}}{T+\alpha} - 1 \right) , \tag{4.74}$$

which exhibits two contradictory dependences on T. The evolution of $I_{\rm out}$ versus T for fixed values of $g_0 L_{\rm a}$ and α is plotted in Figure 4.8. The laser oscillates for $0 \leq T \leq T_{\rm max} = g_0 L_{\rm cav} - \Upsilon$. The maximum output power $I_{\rm out}^{\rm max}$ is obtained for the optimal transmission $T_{\rm opt}$. They are given by:

$$T_{\rm opt} = \sqrt{g_0 L_{\rm a} \alpha} - \alpha \, , \tag{4.75}$$

$$I_{\rm out}^{\rm max} = I_{\rm sat} \Big(\sqrt{g_0 L_{\rm a}} - \sqrt{\alpha} \Big)^2 . \tag{4.76}$$

In the limit where the pumping is very strong and the laser is far above threshold ($\alpha_0 L_{\rm a} \gg \Upsilon$), the maximum laser output power is given by:

$$P_{\rm out}^{\rm max} \simeq S I_{\rm sat} g_0 L_{\rm a} = \frac{\hbar\omega \Delta N_0}{\tau} \, . \tag{4.77}$$

We can thus see that the maximum power that one can extract from the laser medium is equal to the energy that can be stored in the active medium ($\hbar\omega\Delta N_0$) divided by the gain recovery time τ.

The non monotonic evolution of $I_{\rm out}$ versus T shown in Figure 4.8 is yet another consequence of the intrinsic nonlinearity of the laser due to gain saturation.

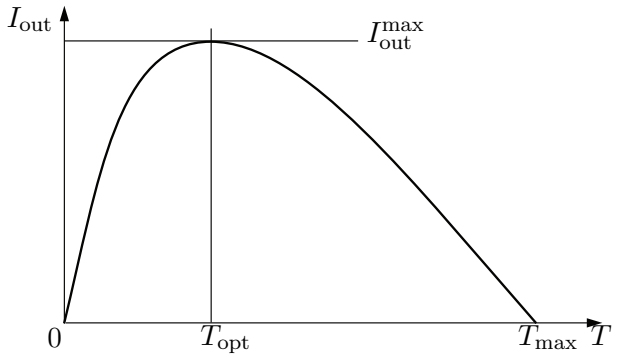

Figure 4.8: Output laser intensity versus output coupler transmission T.

4.2.2 Laser oscillation frequency

a. Cavity modes. Frequency pulling

In Section 4.1.1, we supposed that we could neglect the refractive index of the active medium filling the laser cavity, and we assumed that $\mathrm{e}^{\mathrm{i}k' L_{\rm cav}} = 1$ in the self-consistency Equation (4.4) by taking

$$\omega = \omega_q \equiv q\,\Omega_{\rm cav}\ , \tag{4.78}$$

where q is an integer and the cavity free spectral range is defined in Equation (3.20). The laser frequency is then just simply equal to one of the resonance frequencies of the "cold" cavity studied in Complement 3A. Let us now examine the frequency shift introduced by the real part of the susceptibility of the active medium (see Section 2.3.4). The self-consistency of the phase of the field after one round-trip inside the cavity imposes

$$k'\,L_{\rm cav} = 2q\,\pi\ , \tag{4.79}$$

where we have supposed that the active medium fills the cavity. Using Equation (2.95), we get:

$$\frac{\omega}{c}\left(1+\frac{\chi'}{2}\right) L_{\rm cav} = 2q\,\pi\ . \tag{4.80}$$

The frequency ω of the laser is thus given by:

$$\frac{\omega}{2\pi}\left(1+\frac{\chi'(\omega)}{2}\right) = q\frac{c}{L_{\rm cav}} = \frac{\omega_q}{2\pi}\ . \tag{4.81}$$

Let us suppose that the active medium of the laser can be well described by Lamb's model. Then, using Equations (2.88) and (2.102):

$$\chi'(\omega) = -\frac{\omega-\omega_0}{\Delta\omega/2}\ \chi''(\omega) = \frac{\omega-\omega_0}{\Delta\omega/2}\frac{c}{\omega}\,g(\omega)\ , \tag{4.82}$$

where $\Delta\omega$ is the power broadened full width at half maximum of the gain curve (see Section 2.1.2):

$$\Delta\omega = 2\sqrt{\Gamma_{\rm D}^2 + \Omega_1^2}\,. \tag{4.83}$$

If we suppose that ω is close to ω_q, the frequency shift created by the amplifying atoms reads

$$\omega - \omega_q \simeq \frac{\omega_0 - \omega_q}{\Delta\omega}\frac{c}{\omega}\,g(\omega_q)\,. \tag{4.84}$$

We can thus see that the frequency shift is respectively positive or negative depending whether ω_q is smaller or larger than the center frequency ω_0 of the transition. The active medium thus "pulls" the frequency ω towards the gain maximum: this is the so-called "frequency pulling" effect.

In the case where the active medium has a length $L_{\rm a}$ and does not completely fill the cavity, Equation (4.84) becomes:

$$\frac{\omega - \omega_q}{\omega_q} \simeq \frac{\omega_0 - \omega_q}{\Delta\omega}\frac{c}{\omega}\frac{L_{\rm a} g(\omega_q)}{L_{\rm cav}}\,. \tag{4.85}$$

Let us introduce the quality factors $Q_{\rm cav}$ and $Q_{\rm a}$ for the cavity and the active medium, respectively:

$$Q_{\rm cav} = \omega\,\tau_{\rm cav} = \frac{\omega}{c}\frac{L_{\rm cav,opt}}{\Upsilon}\,, \tag{4.86}$$

$$Q_{\rm a} = \frac{\omega_0}{\Delta\omega}\,. \tag{4.87}$$

Equation (4.85) then reads:

$$\omega = \frac{Q_{\rm cav}\omega_q + Q_{\rm a}\omega_0}{Q_{\rm cav} + Q_{\rm a}}\,. \tag{4.88}$$

The laser frequency is thus the average of the eigenfrequencies of the atoms and the cavity, weighted by their respective quality factors. In many lasers, one has $Q_{\rm cav} \gg Q_{\rm a}$, and the laser frequency is very close to the cavity resonance frequency: $\omega \simeq \omega_q$.

b. Phase of the field

Equation (4.79) has allowed us to determine the frequency of the intra-cavity field. However, it does not impose the phase of the field, i.e., the argument of $\mathcal{A}$. Consequently, one can see that *the phase of the field can take any value*. When the laser is turned on, the field builds up over spontaneously emitted light that can have any phase, and is further amplified by the phase preserving stimulated emission. If one switches the laser off and starts the same experiment again, the laser will reach the same intensity and frequency but a different phase.

4.2.3 Laser threshold and phase transition. Spontaneous symmetry breaking

There is a strong analogy, initially introduced by De Giorgio and Scully[4], between the starting-up of laser oscillation when the unsaturated gain g_0 is larger than the threshold gain, and phase transition phenomena. Indeed, let us consider a ferromagnetic material close to its Curie temperature T_c. Following Weiss law, the magnetization $\mathbf{M}$ depends on the temperature T according to4:

$$c(T - T_c)\mathbf{M} + g\,T\|\mathbf{M}\|^2\,\mathbf{M} = 0\ , \tag{4.89}$$

where g and c are positive constants. When $T > T_c$, the only possible solution is $\mathbf{M} = 0$. When $T < T_c$, the material acquires a magnetization $\mathbf{M}$ such that:

$$\|\mathbf{M}\|^2 = \frac{c(T_c - T)}{g}\ . \tag{4.90}$$

The critical temperature T_c corresponds to a phase transition characterized by the emergence of a *spatial order* for all the microscopic magnetic dipoles. This order corresponds to a non zero so-called order parameter $\mathbf{M}$ (see Figure 4.9).

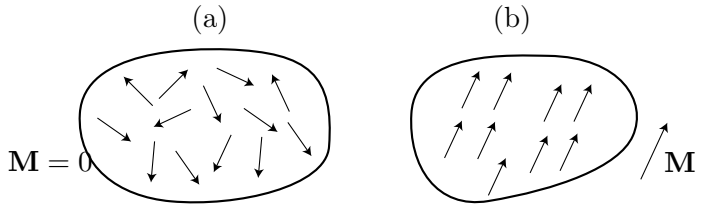

Figure 4.9: Spontaneous symmetry breaking in a ferromagnetic material. (a) Above the Curie temperature, the microscopic magnetic dipoles have random orientations, leading to a vanishing macroscopic magnetization. (b) Below the Curie temperature, the microscopic dipole coupling overcomes the thermal fluctuations, leading to a macroscopic magnetization $\mathbf{M}$. Without any external magnetic field, there is no preferred orientation for $\mathbf{M}$. When the system is cooled down below the Curie temperature, it acquires a magnetization along a particular orientation.

It is worth noticing that Equation (4.89) determines the amplitude of $\mathbf{M}$ only: it does not impose any orientation for $\mathbf{M}$. However, a given sample always chooses an orientation for $\mathbf{M}$: this phenomenon is called a *spontaneous symmetry breaking*. Such a phenomenon *seems to contradict Curie's principle*, according to which the solutions of a problem have the same symmetries as the initial data.

[4] V. De Giorgio and M.O. Scully, *Analogy between the Laser threshold Region and a Second-Order Phase Transition*, Physical Review A2, 1170 (1970). See also M. Sargent, M. O. Scully, W.E. Lamb, *Laser Physics*, Addison-Wesley (1974)

It is possible to reconcile the two points of view by considering that the solution of (4.89) is actually a vectorial *random variable*, which has a deterministic modulus, given by Equation (4.90), but a random direction equally distributed along all possible directions. A given sample must then be considered as a particular realization of a random process. Actually, the whole statistical ensemble obeys Curie's law.

These considerations can be readily transposed to the case of the laser, whose equations are invariant under a transformation $\mathcal{A} \to \mathcal{A}e^{i\varphi}$. Thus the search for steady-state solutions fixes the modulus A of the complex amplitude $\mathcal{A}$, but not its phase ϕ (see Figure 4.10). However, the classical picture of a laser above threshold attributes a modulus A and a phase ϕ to the excited mode: the complex amplitude $\mathcal{A}$ plays the role of the order parameter. The existence of a particular phase for a given laser is due to a spontaneous symmetry breaking, i.e. to a process that violates Curie's law.

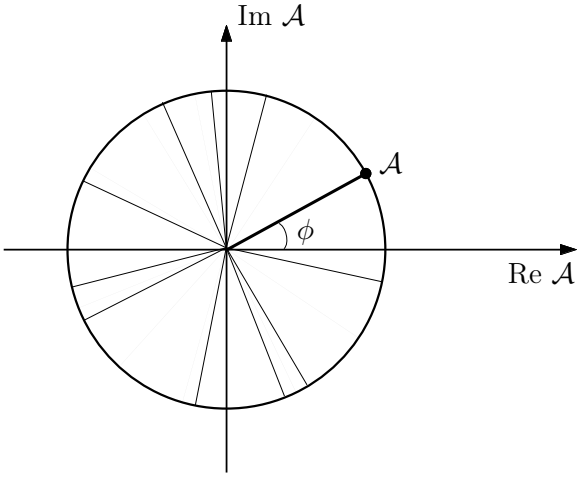

Figure 4.10: Statistical representation of the complex amplitude $\mathcal{A}$ of the laser field considered as a random variable of fixed modulus and random phase equally distributed along $[0, 2\pi]$. A particular sample is represented as a point on the circle.

Like in the case of magnetism, it is possible to reconcile the existence of a phase with the symmetry of the problem by describing the complex amplitude of the laser mode as a complex random variable of fixed modulus, but with a random phase equally distributed along $[0, 2\pi]$ (see Figure 4.10). A laser in a given operation regime corresponds to a particular sample of a statistical ensemble.

4.2.4 Laser power around threshold

The laser oscillation starts from spontaneous emission that is emitted in the laser mode. If we wanted to include the effect of spontaneous emission to our

description, we must use the tools of quantum optics, which will be discussed only in PHY562, and proceed to a fully quantum description of the laser. However, one can introduce spontaneous in a heuristic manner in the present semi-classical description. Indeed, one important result of the fully quantized description of atom-light interaction is that the spontaneous emission falling into the laser mode corresponds to an emission rate which would be the one of stimulated emission induced by the field of one photon inside the cavity. More precisely, we will show that, on statistical average, spontaneous emission can be accounted for in the semi-classical equations of evolution by adding 1 to $\mathcal{N}$ in the expression of the emission rate. Consequently, in the case of a laser based on a four-level system, we replace Equation (4.39) by

$$\frac{\mathrm{d}\mathcal{N}}{\mathrm{d}t} = -\frac{\mathcal{N}}{\tau_{\mathrm{cav}}} + \kappa\Delta N(\mathcal{N}+1) = \kappa[\Delta N(\mathcal{N}+1) - \Delta N_{\mathrm{th}}]\,\mathcal{N}\ . \tag{4.91}$$

In steady-state regime, this leads to:

$$\frac{\Delta N}{\Delta N_{\mathrm{th}}} = \frac{\mathcal{N}}{\mathcal{N}+1}\ . \tag{4.92}$$

Besides, the saturation of the active medium reads

$$\frac{\Delta N}{\Delta N_0} = \frac{1}{1+\mathcal{N}/\mathcal{N}_{\mathrm{sat}}}\ , \tag{4.93}$$

with

$$\mathcal{N}_{\mathrm{sat}} = \frac{1}{\kappa\tau}\ . \tag{4.94}$$

Defining the excitation ratio as $r = \Delta N_0/\Delta N_{\mathrm{th}}$ and combining Equations (4.92) and (4.93), one obtains:

$$\frac{\mathcal{N}}{\mathcal{N}_{\mathrm{sat}}} = \frac{r-1}{2} + \sqrt{\left(\frac{r-1}{2}\right)^2 + \frac{r}{\mathcal{N}_{\mathrm{sat}}}}\ . \tag{4.95}$$

Output power	$P = 100$ mW
Wavelength	$\lambda = 1.06\,\mu$m
Photon flux	$\Pi_{\mathrm{phot}} = P/(hc/\lambda) = 5.3\times10^{16}$ photons/s
Cavity length	$L_{\mathrm{cav}} = 0.4$ m
Mirror transmission (no other losses)	$T = 2\%$
Photon lifetime	$\tau_{\mathrm{cav}} = L_{\mathrm{cav}}/cT = 6.7\times10^{-8}$ s
Number of photons in the cavity	$\mathcal{N} = \tau_{\mathrm{cav}}\Pi_{\mathrm{phot}} = 3.5\times10^{10}$

Table 4.2: Characteristics of a typical Nd:YAG laser

The relative weight of the two terms in the square root in Equation (4.95) determines the evolution of the number of photons in the vicinity of

the laser threshold. It thus strongly depends on the order of magnitude of $\mathcal{N}_{\rm sat}$. To determine this order of magnitude, we take the example of a Nd:YAG laser whose characteristics are given in Table 4.2. Since one has, far above threshold, $\mathcal{N} = \mathcal{N}_{\rm sat}(r-1)$, the order of magnitude of $\mathcal{N}_{\rm sat}$ is thus 10^{10} photons.

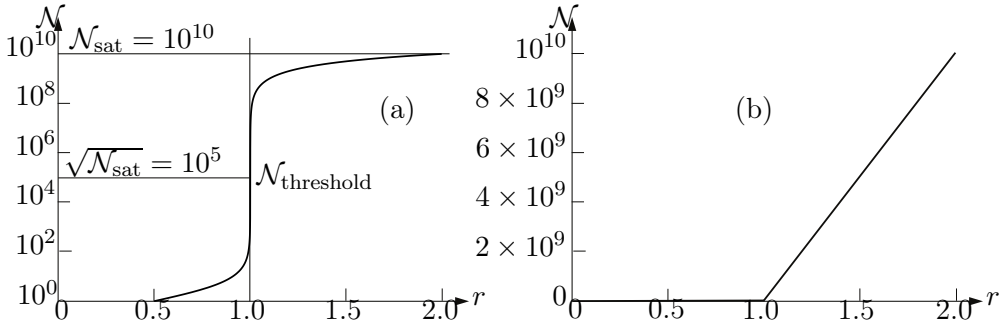

Figure 4.11: Number of photons $\mathcal{N}$ in the cavity versus excitation ratio r for $\mathcal{N}_{\rm sat} = 10^{10}$ plotted on (a) a logarithmic scale and (b) a linear scale.

Figure 4.11(a) reproduces, in a semi-log scale, the evolution of the number of intra-cavity photons versus r for $\mathcal{N}_{\rm sat} = 10^{10}$, plotted using Equation (4.95). *The threshold corresponds to a dramatic increase of* $\mathcal{N}$, with a slope equal to $\mathcal{N}_{\rm sat}/2$. For comparison, the same quantity is plotted on a linear scale in Figure 4.11(b), showing no visible difference with Figure 4.5(b).

Comments

(i) The typical number $(10^{10} - 10^{12})$ of photons in the laser mode that we have obtained explains the remarkable properties of lasers. If one remembers that a "classical" source such as a thermal source with a maximum emission in the visible has much less than one photon per mode, it becomes clear that lasers are indeed extraordinary light sources, in particular as far as spatial and temporal coherence properties are concerned (see Complements 3C and 5A and the conclusion of Chapter 3).

(ii) If one makes $\mathcal{N}_{\rm sat}$ infinite in equation (4.95), one finds $\mathcal{N} = 0$ for $r < 1$, and $\mathcal{N} = (r-1)\mathcal{N}_{\rm sat}$ for $r \geq 1$: the cross-over around the threshold is replaced by a discontinuity of the derivative. Following the analogy with a phase transition, the limit $\mathcal{N}_{\rm sat}$ infinite while keeping r constant can be considered the thermodynamics limit.

4.2.5 Spatial hole burning in a linear cavity

Up to now in this chapter, we have always assumed that the lasing intracavity mode was a traveling plane wave. However, this is possible only in a ring cavity in which one forces unidirectional oscillation. In a so-called "linear" cavity such as the one of Figure 4.12, light bounces back and forth

and creates a standing wave. Contrary to the case of the traveling wave, the light energy density is no longer homogeneous along the propagation axis, leading to a drastic modification of the saturation of the active medium and of the behaviour of the laser.

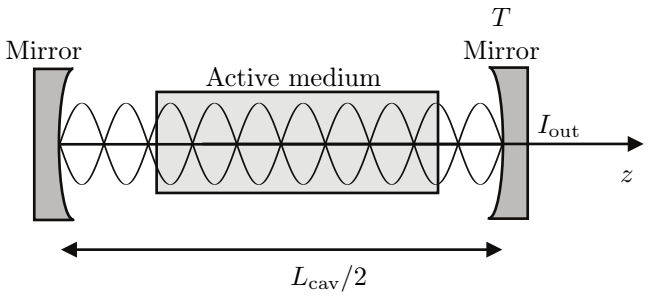

Figure 4.12: Laser based on a linear cavity sustaining standing waves.

a. Standing wave. Saturation

If there were no interferences between the two intra-cavity counter propagating traveling waves of intensities I_+ and I_-, the total intra-cavity intensity would be $I_+ + I_-$, which is close to $2I$ if the losses are small and $I_+ \simeq I_- \simeq I$. The laser steady-state regime could then be described by considering that this total intensity saturates the gain. But the interferences create a spatial modulation of the intensity $I_{\text{sw}}(z)$ along z, and thus the saturation of the population inversion depends on z (this is the so-called spatial hole burning effect). Consequently, we can non longer describe the active medium using the total population inversion ΔN integrated over the laser mode volume inside the active medium, but rather the population inversion density Δn. The saturation of population inversion must then be treated locally along z, leading to:

$$\frac{\Delta n(z)}{\Delta n_0} = \frac{1}{1 + \frac{I_{\text{sw}}(z)}{I_{\text{sat}}}} \ , \tag{4.96}$$

with

$$I_{\text{sw}}(z) = 4I \sin^2(kz) \ . \tag{4.97}$$

b. Output power

The steady-state regime of the laser can be derived by equating the gain and the losses per unit time. Contrary to the traveling wave lasers considered above, the intensity of the standing wave laser depends on z. Instead of the intensity, we thus have to consider the gain and losses of the total electromagnetic energy $\mathcal{W}$ stored inside the cavity. The time variation, due to the

gain, of $\mathcal{W}$ reads[5]:

$$\frac{\mathrm{d}\mathcal{W}}{\mathrm{d}t}\Big|_{\text{gain}} = \varepsilon_0 c\,\sigma_{\text{L}} S \int_0^{L_{\text{a}}} \frac{\Delta n_0 I_{\text{sw}}(z)}{1 + I_{\text{sw}}(z)/I_{\text{sat}}} \mathrm{d}z \ . \tag{4.98}$$

By using Equation (4.97), we obtain, after integration along z:

$$\frac{\mathrm{d}\mathcal{W}}{\mathrm{d}t}\Big|_{\text{gain}} = \varepsilon_0 c\,\sigma_{\text{L}} S \Delta n_0 I_{\text{sat}} L_{\text{a}} \left(1 - \frac{1}{\sqrt{1 + 4I/I_{\text{sat}}}}\right) \ . \tag{4.99}$$

In steady-state regime, this gain must exactly compensate the losses given by:

$$\frac{\mathrm{d}\mathcal{W}}{\mathrm{d}t}\Big|_{\text{losses}} = \frac{2\varepsilon_0 I V_{\text{cav}}}{\tau_{\text{cav}}} \ , \tag{4.100}$$

leading to:

$$\frac{I}{I_{\text{sat}}} = \frac{r}{2}\left(1 - \frac{1}{\sqrt{1 + 4u/u_{\text{sat}}}}\right) \ . \tag{4.101}$$

This third order polynomial equation can be exactly solved. By keeping only the physically meaningful solution we get:

$$I = \frac{I_{\text{sat}}}{2}\left(r - \frac{1}{4} - \sqrt{\frac{r}{2} + \frac{1}{16}}\right) \ . \tag{4.102}$$

Finally, the laser output intensity is given by

$$I_{\text{out}} = \frac{T}{2} I_{\text{sat}} \left(r - \frac{1}{4} - \sqrt{\frac{r}{2} + \frac{1}{16}}\right) \ . \tag{4.103}$$

This result must be compared with the expression (4.74) of the laser output intensity in the absence of spatial hole burning:

$$I_{\text{out}} = \frac{T}{2} I_{\text{sat}} (r - 1) \ . \tag{4.104}$$

This comparison shows that spatial hole burning does not modify the laser threshold, but decreases the slope of its output power characteristics. This is due to the fact that the standing wave does not optimally extract the energy out of the active medium.

The identity of the laser threshold for traveling and standing waves is a signature of the fact that the laser threshold depends only on the *linear* characteristics of the laser, namely its unsaturated gain and its losses. On the contrary, when the laser is above threshold, *nonlinear* saturation plays a role and the laser poser depends on the nature of the intracavity wave .

[5]To write Equation (4.98), we have supposed that gain saturation is instantaneous. This hypothesis is not valid in all kinds of lasers. We will come back to this point in Section 4.3 and in Chapter 5.

4.3 Laser dynamic classes. Adiabatic elimination of the active medium

In Section 4.1, we have established the equations of evolution for the single frequency laser:

$$\frac{\mathrm{d}\mathcal{N}}{\mathrm{d}t} = -\frac{\mathcal{N}}{\tau_{\mathrm{cav}}} + \kappa\,\Delta N\,\mathcal{N}\,, \tag{4.105}$$

$$\frac{\mathrm{d}\Delta N}{\mathrm{d}t} = \Gamma(\Delta N_0 - \Delta N) - 2^*\kappa\,\Delta N\,\mathcal{N}\,. \tag{4.106}$$

The different notations are defined in Section 4.1.

An important feature of Equations (4.105) and (4.106) is the presence of the relaxation terms $-\mathcal{N}/\tau_{\mathrm{cav}}$ and $-\Gamma\Delta N$ which govern the relaxation of the system towards its steady-state solutions. Depending on the relative values of the times $\tau = 1/\Gamma$ and τ_{cav}, two dynamical classes of lasers can be distinguished:

• Case where $\tau_{\mathrm{cav}} \gg 1/\Gamma$: class-A laser

Most gas lasers and dye lasers belong to this class. In this case, the relaxation time $1/\Gamma$ of the population inversion is so short that we can consider that ΔN always adjusts to the steady-state solution of Equation (4.106), even if $\mathcal{N}$ (slowly) varies. Indeed, let us suppose that $\mathcal{N}$ is equal to a constant $\mathcal{N}_0$ and that ΔN takes an initial value ΔN_0 at $t = 0$. Then, using Equation (4.106), the further evolution of $\Delta N(t)$ is given by:

$$\Delta N(t) = \frac{\Delta N_0}{1 + \frac{2^*\kappa}{\Gamma}\mathcal{N}_0}\left(1 - \mathrm{e}^{-\Gamma t}\right)\,. \tag{4.107}$$

This shows that ΔN reaches its steady-state value on a timescale of the order of $1/\Gamma$. From the structure of Equation (4.105), we can see that $\mathcal{N}$ evolves on a time scale of the order of τ_{cav}. Since $\tau_{\mathrm{cav}} \ll 1/\Gamma$, we can thus consider that, from the point of view of ΔN, $\mathcal{N}$ is static, and Δ will reach its steady-state value at every instant. Consequently, we can *adiabatically eliminate* ΔN, meaning that we suppose that $\mathrm{d}\Delta N/\mathrm{d}t = 0$ at all instants in Equation (4.106), leading to:

$$\Delta N(t) = \frac{\Delta N_0}{1 + \frac{2^*\kappa}{\Gamma}\mathcal{N}(t)}\,. \tag{4.108}$$

Gain saturation is thus instantaneous compared to the time scale of the variations of $\mathcal{N}(t)$. Injecting (4.108) into (4.105), we are left with

$$\frac{\mathrm{d}\mathcal{N}}{\mathrm{d}t} = -\frac{\mathcal{N}}{\tau_{\mathrm{cav}}} + \frac{\kappa\,\Delta N_0\,\mathcal{N}}{1 + \frac{2^*\kappa}{\Gamma}\mathcal{N}(t)} = -\frac{\mathcal{N}}{\tau_{\mathrm{cav}}} + \frac{\kappa\,\Delta N_0\,\mathcal{N}}{1 + \mathcal{N}/\mathcal{N}_{\mathrm{sat}}}\,, \tag{4.109}$$

with $\mathcal{N}_{\mathrm{sat}} = \Gamma/2^*\kappa$.

This equation simply states that the evolution of the number of photons is due to the losses and the saturated gain. Equation (4.109) could equally be written for the intensity:

$$\frac{\mathrm{d}I}{\mathrm{d}t} = -\frac{I}{\tau_{\mathrm{cav}}} + \frac{\kappa\,\Delta N_0 I}{1 + I/I_{\mathrm{sat}}}\,, \tag{4.110}$$

or for the field complex amplitude:

$$\begin{aligned}\frac{\mathrm{d}\mathcal{A}}{\mathrm{d}t} &= -\frac{\mathcal{A}}{2\tau_{\mathrm{cav}}} + \frac{\kappa\Delta N_0}{2}\frac{\mathcal{A}}{1 + 2|\mathcal{A}|^2/I_{\mathrm{sat}}} \\ &= \frac{\mathcal{A}}{2\tau_{\mathrm{cav}}}\left(\frac{r}{1 + 2|\mathcal{A}|^2/I_{\mathrm{sat}}}\right)\,,\end{aligned} \tag{4.111}$$

where we have used the definition of r given in Equation 4.55.

Using Equation (4.17), (4.18), and (4.54), this equation can be re-written for the number of photons inside the cavity in the following form:

$$\frac{\mathrm{d}\mathcal{N}}{\mathrm{d}t} = \frac{\mathcal{N}}{\tau_{\mathrm{cav}}}\left(\frac{r}{1 + \mathcal{N}/\mathcal{N}_{\mathrm{sat}}}\right)\,. \tag{4.112}$$

By taking $\mathrm{d}\mathcal{N}/\mathrm{d}t$ in this equation, one immediately obtains the steady-state solutions $\mathcal{N}_{\mathrm{OFF}}$ and $\mathcal{N}_{\mathrm{ON}}$ (see Equations 4.51 and 4.53) that were derived in Section 4.2.1.

• Case where $\tau_{\mathrm{cav}} \sim 1/\Gamma$ or $\tau_{\mathrm{cav}} < 1/\Gamma$: class-B laser

The ruby, Nd:YAG, Er:glass, diode lasers, and some CO_2 lasers belong to this class. In this case one cannot perform the adiabatic elimination of ΔN. We are thus left with the two Equations (4.105) and (4.106).

The distinction between class-A and class-B lasers does not impact the steady-state solutions of the laser and their stability that we have studied in section 4.2. However, as we will see in chapter 5, it plays an important role on the dynamical behaviour of the laser.

Comments

(i) In the case of the class-B laser with $\tau_{\mathrm{cav}} \ll 1/\Gamma$, one could wonder whether it could not be possible to adiabatically eliminate the variable $\mathcal{N}$ by setting $\frac{\mathrm{d}\mathcal{N}}{\mathrm{d}t} = 0$ in Equation (4.105) and keep only one equation of evolution for ΔN. However, the absence of a term equivalent to $\Gamma\Delta N_0$ in Equation (4.105) forbids this simplification.

(ii) There exists another very rare dynamical class of lasers, the so-called class-C laser, which corresponds to the case where the atomic dipole cannot be adiabatically eliminated and the full dynamics of the atomic system must be kept. One then has three differential equations instead of two, as described in Complement 4A. Such lasers can exhibit surprising dynamical behaviors, such as deterministic chaos.

4.4 Two-frequency lasers: mode competition

Up to now, we have considered almost exclusively single-frequency lasers. We have seen in particular in Section 3.3.2 that in the ideal case of a laser based on a homogeneously broadened active medium and a unidirectional ring cavity, *mode competition* leads to single-frequency operation. This is a marginal situation and we have already mentioned several cases in which this approximation is not valid. In this section, we will suppose that the laser, thanks for example to the fact that the active medium exhibits some inhomogeneous broadening, can sustain the oscillation of two modes with two different frequencies. It is beyond the scope of the present chapter to derive a general theory for mode competition. We will content ourselves by introducing a simple model for mode competition and analyzing its consequences on the steady-state behaviour of two-modes lasers.

4.4.1 Self- and cross-saturation terms

In general, the problem of gain saturation in two-mode lasers is very complicated[6]. Our aim here is to heuristically introduce the minimum of formalism leading to the correct description of the physical phenomena observed in actual systems. Let us consider a laser sustaining the oscillation of two modes labeled 1 and 2. These two modes can be two different longitudinal modes, two different transverse modes, two counterpropagating modes in a ring laser, or two different polarization modes. We note $\mathcal{N}_1$ and $\mathcal{N}_2$ the numbers of photons of these two modes, and we suppose that these two modes take their gains from two *independent* population inversion reservoirs ΔN_1 and ΔN_2. This would be for example the case of two different longitudinal modes that burn well separated spectral holes in an in homogeneously broadened medium like in Figure 3.7. Then the rate equations for this laser read:

$$\frac{\mathrm{d}\mathcal{N}_1}{\mathrm{d}t} = -\frac{\mathcal{N}_1}{\tau_{\mathrm{cav}1}} + \kappa_1 \mathcal{N}_1 \Delta N_1 \ , \tag{4.113}$$

$$\frac{\mathrm{d}}{\mathrm{d}t}\Delta N_1 = \Gamma(\Delta N_{01} - \Delta N_1) - 2^* \kappa_1 \mathcal{N}_1 \Delta N_1 \ , \tag{4.114}$$

$$\frac{\mathrm{d}\mathcal{N}_2}{\mathrm{d}t} = -\frac{\mathcal{N}_2}{\tau_{\mathrm{cav}2}} + \kappa_2 \mathcal{N}_2 \Delta N_2 \ , \tag{4.115}$$

$$\frac{\mathrm{d}}{\mathrm{d}t}\Delta N_2 = \Gamma(\Delta N_{02} - \Delta N_2) - 2^* \kappa_2 \mathcal{N}_2 \Delta N_2 \ , \tag{4.116}$$

where we have supposed that the two modes may have two different photon lifetimes and exhibit two different laser cross sections and pumping rates.

[6] See for example M. Sargent, M. O. Scully, W.E. Lamb, *Laser Physics*, Addison-Wesley (1974)

Equations (4.113, 4.114) and (4.115, 4.116) constitute two completely independent sets of equations, as if the two modes were actually oscillating in two different lasers. If we want to take into account the possible competition of the two modes for gain, we can suppose that each population inversion ΔN_i with $i = 1, 2$ is subjected not only to *self-saturation* terms such as $2^*\kappa_i \mathcal{N}_i \Delta N_i$ but also to *cross-saturation* terms $2^*\kappa_i \xi_{ij} \mathcal{N}_j \Delta N_i$, leading to:

$$\frac{\mathrm{d}\mathcal{N}_1}{\mathrm{d}t} = -\frac{\mathcal{N}_1}{\tau_{\mathrm{cav1}}} + \kappa_1 \mathcal{N}_1 \Delta N_1 \ , \tag{4.117}$$

$$\frac{\mathrm{d}}{\mathrm{d}t}\Delta N_1 = \Gamma(\Delta N_{01} - \Delta N_1) - 2^*\kappa_1 \Delta N_1 (\mathcal{N}_1 + \xi_{12}\mathcal{N}_2) \ , \tag{4.118}$$

$$\frac{\mathrm{d}\mathcal{N}_2}{\mathrm{d}t} = -\frac{\mathcal{N}_2}{\tau_{\mathrm{cav2}}} + \kappa_2 \mathcal{N}_2 \Delta N_2 \ , \tag{4.119}$$

$$\frac{\mathrm{d}}{\mathrm{d}t}\Delta N_2 = \Gamma(\Delta N_{02} - \Delta N_2) - 2^*\kappa_2 \Delta N_2 (\mathcal{N}_2 + \xi_{21}\mathcal{N}_1) \ , \tag{4.120}$$

The ratios ξ_{12} and ξ_{12} of the cross- to self-saturation coefficients that we have introduced here can take any positive value[7]. Let us repeat once more that this is the simplest way to introduce mode competition and that in real situations, extra terms must also usually be added to Equations (4.117) and (4.119). However, the presence of both self- and cross-saturation terms in these equations makes them even more nonlinear than before and we can thus expect new phenomena to occur.

4.4.2 Restriction to the case of class-A lasers

If we restrict to a class-A laser, Equations (4.118) and (4.120) can be adiabatically eliminated, leading to:

$$\Delta N_1 = \frac{\Delta N_{01}}{1 + (\mathcal{N}_1 + \xi_{12}\mathcal{N}_2)/\mathcal{N}_{\mathrm{sat1}}} \ , \tag{4.121}$$

$$\Delta N_2 = \frac{\Delta N_{02}}{1 + (\mathcal{N}_2 + \xi_{21}\mathcal{N}_1)/\mathcal{N}_{\mathrm{sat2}}} \ , \tag{4.122}$$

with

$$\mathcal{N}_{\mathrm{sat1}} = \frac{\Gamma}{2^*\kappa_1} \ , \tag{4.123}$$

$$\mathcal{N}_{\mathrm{sat2}} = \frac{\Gamma}{2^*\kappa_2} \ . \tag{4.124}$$

[7] ξ_{12} and ξ_{12} cannot be negative because that would mean that saturation by one mode increases the gain of the other mode.

The laser behaviour is then governed by the two remaining equations:

$$\frac{\mathrm{d}\mathcal{N}_1}{\mathrm{d}t} = \frac{\mathcal{N}_1}{\tau_{\mathrm{cav}1}}\left[-1 + \frac{r_1}{1 + (\mathcal{N}_1 + \xi_{12}\mathcal{N}_2)/\mathcal{N}_{\mathrm{sat}1}}\right] , \tag{4.125}$$

$$\frac{\mathrm{d}\mathcal{N}_2}{\mathrm{d}t} = \frac{\mathcal{N}_2}{\tau_{\mathrm{cav}2}}\left[-1 + \frac{r_2}{1 + (\mathcal{N}_2 + \xi_{21}\mathcal{N}_1)/\mathcal{N}_{\mathrm{sat}2}}\right] , \tag{4.126}$$

where we have introduced the relative excitation ratios $r_i = \tau_{\mathrm{cav}i}\kappa_i\Delta\mathcal{N}_{0i}$ for the two modes $i = 1, 2$.

The physical meaning of these two equations is clear: the evolution of the number of photons in each mode contains two terms, corresponding to losses and gain, respectively. The gain of each mode is saturated by its own number of photons (self-saturation $\mathcal{N}_i/\mathcal{N}_{\mathrm{sati}}$) and by the number of photons in the other mode (cross-saturation $\xi_{ij}\mathcal{N}_j/\mathcal{N}_{\mathrm{sati}}$).

4.4.3 Steady-state solution

We suppose in the following that the two modes are above threshold, meaning that $r_1 > 1$ and $r_2 > 1$. This makes the steady-state solution $\mathcal{N}_1 = \mathcal{N}_2 = 0$ unstable, and we will no longer consider it in the following. The other steady-state solutions are obtained by taking $\dfrac{\mathrm{d}\mathcal{N}_1}{\mathrm{d}t} = \dfrac{\mathrm{d}\mathcal{N}_2}{\mathrm{d}t} = 0$ in Equations (4.125) and (4.126), leading to:

$$(\alpha) \quad \mathcal{N}_1 = 0 \quad \text{or} \quad (\beta) \quad \mathcal{N}_1 + \xi_{12}\,\mathcal{N}_2 = \mathcal{N}_{\mathrm{sat}1}(r_1 - 1) , \tag{4.127}$$

$$(\gamma) \quad \mathcal{N}_2 = 0 \quad \text{or} \quad (\delta) \quad \mathcal{N}_2 + \xi_{21}\,\mathcal{N}_1 = \mathcal{N}_{\mathrm{sat}2}(r_2 - 1) . \tag{4.128}$$

The four equations labelled $(\alpha, \beta, \gamma, \delta)$ correspond to four straight lines in the $(\mathcal{N}_1, \mathcal{N}_2)$ plane, like for example in Figures 4.13, 4.14, and 4.15 that will be discussed below. The steady-state solutions thus correspond to the intersection points between either (α) or (β) on the one hand and either (γ) or (δ) on the other hand. If we eliminate the intersection between (α) and (γ), which is the trivial solution $\mathcal{N}_1 = \mathcal{N}_2 = 0$, we see that we are left with three possible solutions: i) only mode 1 oscillates (intersection of (β) and (γ)); ii) only mode 2 oscillates (intersection of (α) and (δ)); iii) the two modes oscillate simultaneously (intersection of (β) and (δ)). In the following, we discuss the stability of these solutions.

a. The stronger mode takes all

Let us look for the stability domain of the situation for which only one steady-state solution is stable, the one for which only mode 1 oscillates:

$$\mathcal{N}_1^0 = \mathcal{N}_{\mathrm{sat}1}(r_1 - 1) , \tag{4.129}$$

$$\mathcal{N}_2^0 = 0 . \tag{4.130}$$

To evaluate the stability of this solution in a way analogous to Section 4.2b, we rewrite $\mathcal{N}_1(t)$ and $\mathcal{N}_2(t)$ according to:

$$\mathcal{N}_1(t) = \mathcal{N}_1^0 + \delta\mathcal{N}_1(t) \,, \tag{4.131}$$

$$\mathcal{N}_2(t) = \delta\mathcal{N}_2(t) \,. \tag{4.132}$$

By injecting Equations (4.131) and (4.132) into Equations (4.125) and (4.126) with the help of Equations (4.129) and (4.130) and keeping only first-order terms in $\delta\mathcal{N}_1$ and $\delta\mathcal{N}_2$, one obtains:

$$\frac{\mathrm{d}}{\mathrm{d}t}\delta\mathcal{N}_1 = -\frac{\mathcal{N}_1^0}{\tau_{\mathrm{cav}1}} \frac{\delta\mathcal{N}_1 + \xi_{12}\delta\mathcal{N}_2}{r_1\,\mathcal{N}_{\mathrm{sat}1}} \,, \tag{4.133}$$

$$\frac{\mathrm{d}}{\mathrm{d}t}\delta\mathcal{N}_2 = \frac{\delta\mathcal{N}_2}{\tau_{\mathrm{cav}2}} \left(-1 + \frac{r_2}{1 + \xi_{21}\mathcal{N}_1^0/\mathcal{N}_{\mathrm{sat}2}} \right) \,. \tag{4.134}$$

The eigenvalues of the matrix corresponding to Equations (4.133) and (4.134) are both negative when

$$\frac{r_2}{1 + \xi_{21}\mathcal{N}_1^0/\mathcal{N}_{\mathrm{sat}2}} < 1 \,. \tag{4.135}$$

This condition means that the gain of mode 2 saturated by the presence of mode 1 is smaller than the losses, preventing mode 2 from reaching threshold.

Using Equation (4.129), Equation (4.135) can be re-written in the following form:

$$\frac{\mathcal{N}_{\mathrm{sat}2}(r_2 - 1)}{\xi_{21}} < \mathcal{N}_{\mathrm{sat}1}(r_1 - 1) \,. \tag{4.136}$$

Similarly, if we want the solution (4.129–4.130) to be the only stable one, we need the solution in which only mode 2 oscillates to be unstable, leading, in analogy with (4.136) to:

$$\frac{\mathcal{N}_{\mathrm{sat}1}(r_1 - 1)}{\xi_{12}} > \mathcal{N}_{\mathrm{sat}2}(r_2 - 1) \,. \tag{4.137}$$

To illustrate this situation, we consider the four lines corresponding to $(\alpha, \beta, \gamma, \delta)$ in Equations (4.127–4.128). These lines are plotted in Figure 4.13, and steady-state solutions must be intersections of one full line with one dotted line. This figure shows that the inequalities (4.136) and (4.137) lead to the fact that the two lines (β) and (δ) do not cross in the $\mathcal{N}_1, \mathcal{N}_2 \geq 0$ quadrant. The only stable solution is the one corresponding to a circle in Figure 4.13. This situation, which is reminiscent of the discussion of Figure 3.9, corresponds to the case where the stronger mode takes all the gain and "stifles" the weaker mode.

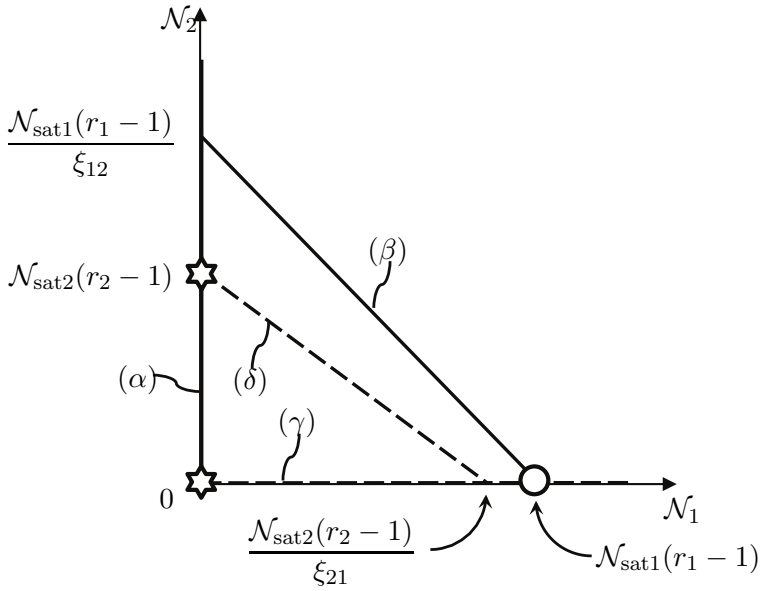

Figure 4.13: Situation where only mode 1 can oscillate. The circle corresponds to the stable steady-state solution and the stars to the unstable ones. The full lines correspond to (α) and (β) in Equation (4.127) while the dashed lines correspond to (γ) and (δ) in Equation (4.128).

b. Simultaneous oscillation of the two modes

Let us now consider the steady-state solution of Equations (4.125) and (4.126) for which $\mathcal{N}_1 \neq 0$ and $\mathcal{N}_2 \neq 0$, i.e. the intersection point of the lines defined by Equations (β) and (γ) in (4.127) and (4.128):

$$\mathcal{N}_1^0 = \frac{\mathcal{N}_{\rm sat1}(r_1-1) - \xi_{12}\mathcal{N}_{\rm sat2}(r_2-1)}{1-\xi_{12}\,\xi_{21}}\,, \tag{4.138}$$

$$\mathcal{N}_2^0 = \frac{\mathcal{N}_{\rm sat2}(r_2-1) - \xi_{21}\mathcal{N}_{\rm sat1}(r_1-1)}{1-\xi_{12}\,\xi_{21}} \tag{4.139}$$

In the absence of mode competition ($\xi_{12} = \xi_{21} = 0$), one recovers for each mode the usual solution of a single-frequency laser above threshold (see Equation 4.53), just like in Figure 4.6.

To study the stability of the solution (4.138, 4.139), we perform a linear stability analysis by writing:

$$\mathcal{N}_1(t) = \mathcal{N}_1^0 + \delta\mathcal{N}_1(t)\,, \tag{4.140}$$

$$\mathcal{N}_2(t) = \mathcal{N}_2^0 + \delta\mathcal{N}_2(t)\,, \tag{4.141}$$

with $|\delta\mathcal{N}_1(t)| \ll \mathcal{N}_1^0$ and $|\delta\mathcal{N}_2(t)| \ll \mathcal{N}_2^0$. By injecting Equations (4.140) and (4.141) into (4.125) and (4.126) and keeping only first-order terms in $\delta\mathcal{N}_1$

and $\delta\mathcal{N}_2$, one obtains:

$$\frac{\mathrm{d}}{\mathrm{d}t}\begin{pmatrix}\delta\mathcal{N}_1\\ \\ \delta\mathcal{N}_2\end{pmatrix} = M\begin{pmatrix}\delta\mathcal{N}_1\\ \\ \delta\mathcal{N}_2\end{pmatrix}\ , \tag{4.142}$$

with

$$M = -\begin{pmatrix}\mathcal{N}_1^0/\tau_{\mathrm{cav}1}r_1\mathcal{N}_{\mathrm{sat}1} & \xi_{12}\mathcal{N}_1^0/\tau_{\mathrm{cav}1}r_1\mathcal{N}_{\mathrm{sat}1}\\ \\ \xi_{21}\mathcal{N}_1^0/\tau_{\mathrm{cav}2}r_2\mathcal{N}_{\mathrm{sat}2} & \mathcal{N}_2^0/\tau_{\mathrm{cav}2}r_2\mathcal{N}_{\mathrm{sat}2}\end{pmatrix}\ . \tag{4.143}$$

The eigenvalues of $-M$ are given by the characteristic equation:

$$\left(\lambda - \frac{\mathcal{N}_1^0}{r_1\tau_{\mathrm{cav}1}\mathcal{N}_{\mathrm{sat}1}}\right)\left(\lambda - \frac{\mathcal{N}_2^0}{r_2\tau_{\mathrm{cav}2}\mathcal{N}_{\mathrm{sat}2}}\right) - \frac{\xi_{12}\xi_{21}\mathcal{N}_1^0\mathcal{N}_2^0}{r_1r_2\tau_{\mathrm{cav}1}\tau_{\mathrm{cav}2}\mathcal{N}_{\mathrm{sat}1}\mathcal{N}_{\mathrm{sat}2}} = 0\ , \tag{4.144}$$

leading to

$$\lambda^2 - \lambda\left(\frac{\mathcal{N}_1^0}{r_1\tau_{\mathrm{cav}1}\mathcal{N}_{\mathrm{sat}1}} + \frac{\mathcal{N}_2^0}{r_2\tau_{\mathrm{cav}2}\mathcal{N}_{\mathrm{sat}2}}\right) + \frac{\mathcal{N}_1^0\mathcal{N}_2^0}{r_1r_2\tau_{\mathrm{cav}1}\tau_{\mathrm{cav}2}\mathcal{N}_{\mathrm{sat}1}\mathcal{N}_{\mathrm{sat}2}}(1-\xi_{12}\xi_{21}) = 0\ . \tag{4.145}$$

The solution given by Equations (4.138) and (4.139) is stable provided the two solutions λ_+ and λ_- of Equation (4.145) have positive real parts. Let us rewrite Equation (4.145) in the following form:

$$\lambda^2 - \lambda(\alpha+\beta) + \alpha\beta(1-C) = 0\ , \tag{4.146}$$

where we have defined

$$\alpha = \frac{\mathcal{N}_1^0}{r_1\tau_{\mathrm{cav}1}\mathcal{N}_{\mathrm{sat}1}}\ , \tag{4.147}$$

$$\beta = \frac{\mathcal{N}_2^0}{r_2\tau_{\mathrm{cav}2}\mathcal{N}_{\mathrm{sat}2}}\ , \tag{4.148}$$

$$C = \xi_{12}\xi_{21}\ . \tag{4.149}$$

The discriminant of Equation (4.146) is

$$\Delta = (\alpha+\beta)^2 - 4\alpha\beta(1-C) = (\alpha-\beta)^2 + 4\alpha\beta C\ . \tag{4.150}$$

The sum and products of the two solutions are given by $\lambda_+ + \lambda_- = \alpha+\beta$ and $\lambda_+\lambda_- = \alpha\beta(1-C)$, respectively. In the case where $\alpha > 0$ and $\beta > 0$, λ_+ and λ_- can be both positive only if $C < 1$. Besides, in the case where $\alpha+\beta > 0$ but one of the numbers α or β is negative (for example $\alpha > 0$ and $-\alpha < \beta < 0$), Equation (4.150) reads

$$\Delta = \alpha^2 + \beta^2 + 2|\alpha\beta| - 4C|\alpha\beta| > \alpha^2 + \beta^2 + 2|\alpha\beta| - 4|\alpha\beta| > 0\ . \tag{4.151}$$

Then λ_+ and λ_- are both real. The stability depends on the sign of

$$\lambda_- = \frac{1}{2}\left\{(\alpha+\beta) - \sqrt{(\alpha+\beta)^2 - 4\alpha\beta(1-C)}\right\} \tag{4.152}$$

which is clearly negative. The simultaneous oscillation of the two modes is then unstable.

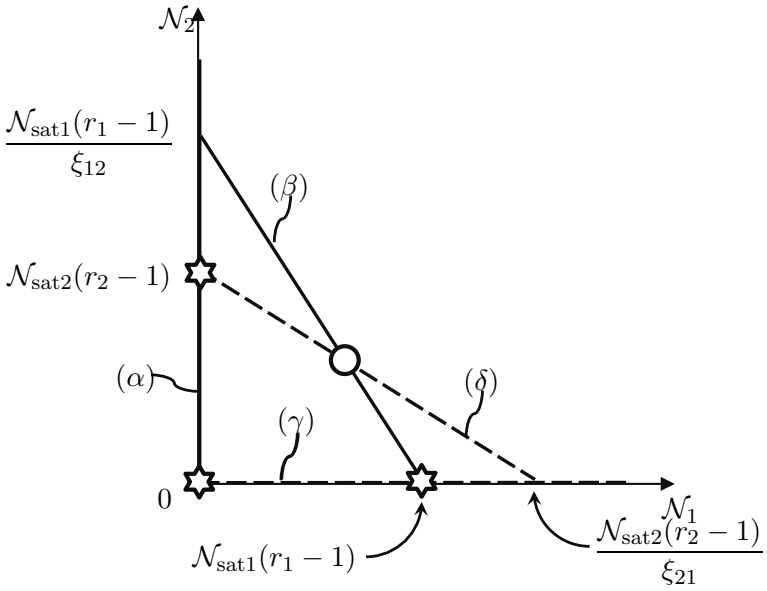

Figure 4.14: Situation where both modes oscillate simultaneously (weak coupling case, $C < 1$). The circle corresponds to the stable steady-state solution and the stars to the unstable ones. The full lines correspond to (α) and (β) in Equation (4.127) while the dashed lines correspond to (γ) and (δ) in Equation (4.128).

In conclusion, the solution given by Equations (4.138) and (4.139), which corresponds to the *simultaneous oscillation of the two modes*, is stable only when the three following conditions are satisfied:

$$\mathcal{N}_1^0 > 0\,, \tag{4.153}$$

$$\mathcal{N}_2^0 > 0\,, \tag{4.154}$$

$$C = \xi_{12}\xi_{21} \leq 1\,. \tag{4.155}$$

Using Equations (4.138) and (4.139), this situation can be represented in the $(\mathcal{N}_1, \mathcal{N}_2)$ plane (see Figure 4.14). The intersection of the two lines (β) and (δ) is the only stable solution, thanks to the fact that the *coupling constant* C is smaller than 1. This situation, where cross-saturation is smaller than self-saturation in Equations (4.125) and (4.126), is called the *weak coupling case*.

The preceding discussion focuses on the intensities of the two modes and does not give any prediction about the relative phase of the two modes when they oscillate simultaneously inside the same laser. When the frequencies of these two modes are well separated, no relative phase locking can occur and the phases are uncorrelated, contrary to what can happen when there are at least three oscillating modes and so-called *mode locking* is possible (see Section 5.3). On the contrary, when the frequency difference between the two modes is small, the two frequencies can lock to each other if a small fraction of the field of one of the modes is injected into the other one. This *injection locking* phenomenon, which is quite similar to the phase locking of coupled mechanical oscillators (Huyghens pendulums) or electronic oscillators, is the subject of Complement 4B.

c. Bistability

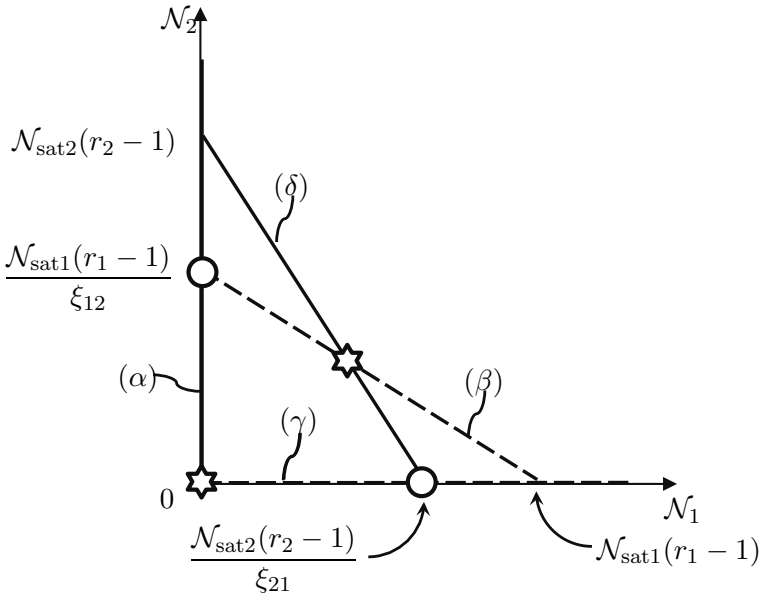

Figure 4.15: Situation where the two-mode laser exhibits bistability (strong coupling case $C > 1$). The circles correspond to the stable steady-state solutions and the stars to the unstable ones. The full lines correspond to (α) and (β) in Equation (4.127) while the dashed lines correspond to (γ) and (δ) in Equation (4.128).

As we have seen in paragraph 4.4.3a above, the condition for stable oscillation of mode 1 alone is given by Equation (4.135). Let us imagine a situation in which this solution is stable and the symmetric solution where only mode 2 oscillates is also stable. Then the two following conditions must

be simultaneously fulfilled:

$$\frac{r_1}{1+\xi_{12}\mathcal{N}_{\rm sat2}(r_2-1)/\mathcal{N}_{\rm sat1}} \leq 1 \ , \tag{4.156}$$

$$\frac{r_2}{1+\xi_{21}\mathcal{N}_{\rm sat1}(r_1-1)/\mathcal{N}_{\rm sat2}} \leq 1 \ . \tag{4.157}$$

These conditions mean that the gain of mode 1 (resp. mode 2) saturated by mode 2 (resp. mode 1) only is lower than the losses, preventing it from oscillating. These equations can be re-written in the following form:

$$\mathcal{N}_{\rm sat2}(r_2-1) \ \geq \ \frac{\mathcal{N}_{\rm sat1}(r_1-1)}{\xi_{12}} \ , \tag{4.158}$$

$$\mathcal{N}_{\rm sat1}(r_1-1) \ \geq \ \frac{\mathcal{N}_{\rm sat2}(r_2-1)}{\xi_{21}} \ , \tag{4.159}$$

showing that the lines (β) and (γ) given by Equations (4.127) and (4.128) look like in Figure 4.15. It is easy to show that Equations (4.158) and (4.159) lead to the following condition on the coupling constant:

$$C = \xi_{12}\xi_{21} \ \geq \ 1 \ . \tag{4.160}$$

This condition also shows that, according to the discussion of paragraph 4.4.3b, the solution corresponding to simultaneous oscillation of the two modes becomes unstable, as evidenced by the star at the intersection of lines (β) and (δ) in Figure 4.15.

The consequences of this situation are better described in Figure 4.16. This figure is a cartoon of what happens when one slowly scans the frequencies of the two modes labeled 1 and 2, which are supposed to have the same losses, across the gain profile. From (a) to (e), the two frequencies are increased, for example by decreasing the cavity length. This can be done by mounting one of the cavity mirrors on a piezoelectric transducer and applying a voltage ramp on this actuator. In (a), only mode 2 is oscillating because mode 1 is below threshold. Then, by increasing the two frequencies, we arrive in (b), where mode 1 is above threshold, but its unsaturated gain is much lower than the one of mode 2, leading to the fact that we are in the situation of Section 4.4.2a: mode 2 takes all the gain and oscillates alone. We then further increase the two frequencies to reach the situation described in (c): now the two modes have the same gain and same losses. It is only the fact that mode 2 was oscillating alone before this point was reached that ensure that it is still oscillating at this point. If one further increases the two frequencies, mode 2 goes on oscillating alone till we reach Figure (d). After this, the bistable solution becomes unstable and the only stable solution corresponds ton the oscillation of mode 1 only: the laser flips from mode 2 to mode 1. It is worth noticing that between points (c) and (d), the mode that

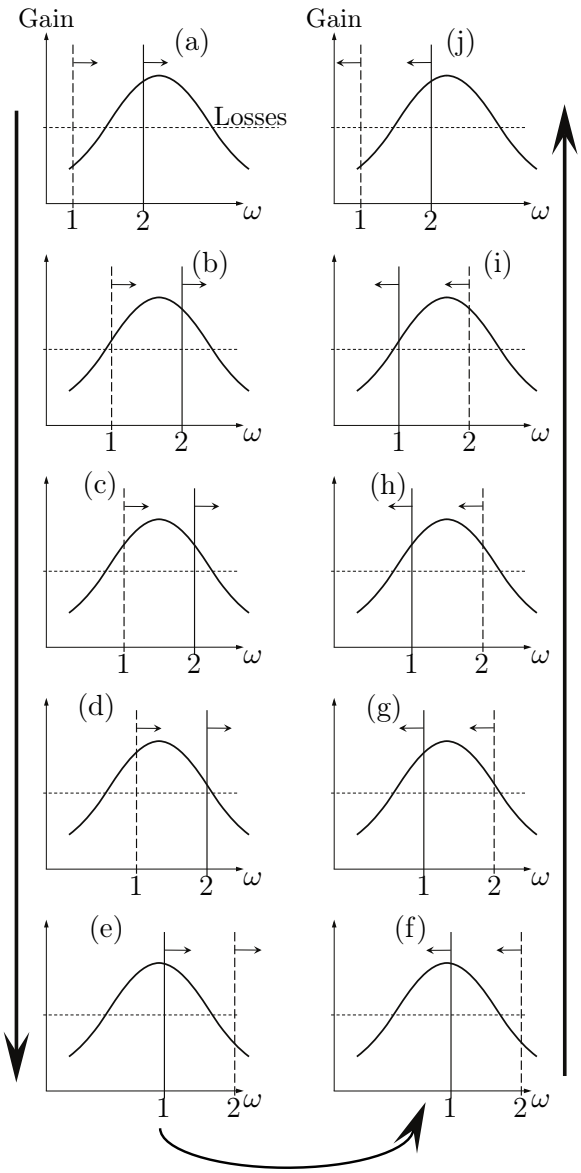

Figure 4.16: (a,b) Evolution of the frequencies of the two modes across the gain profile when the cavity length is scanned in the two opposite directions. (c) Resulting evolution of the number of photons in mode 1 as a function of the cavity length. Mode 2 exhibits the complementary evolution.

oscillates, namely mode 2, is not the mode that has the larger gain. In this domain, the stable solutions correspond to bistability, and the laser follows the same solution (only mode 2 oscillates) by continuity. From (d), if we further decrease the cavity length, mode 2 ends up being below threshold as shown in (e) and mode 1 alone goes on oscillating.

At this point (e), we reverse the direction of the frequency scan, by increasing the cavity length. Further evolution of the laser is cartooned in Figures 4.16(f-j). From (f) to (g), only mode 2 oscillates because it is the only stable solution. From (g) to (i), we are in the bistability domain, where the two modes could oscillate, an only continuity allows us to predict that mode 1 oscillates. In particular, if we compare Figures (c) and (h), we see that the laser parameters are the same in both figures: the two modes are symmetric with respect to the gain medium and thus have exactly the same gain and losses. But the oscillating mode depends on the direction of the frequency scan: mode 2 when the frequencies are increased and mode 1 when they are decreased. Figure (i) corresponds to the point where the gain of mode 1 becomes so weak that the bistable solution becomes unstable, and mode 2 alone becomes stable, till we reach Figure 4.16(j).

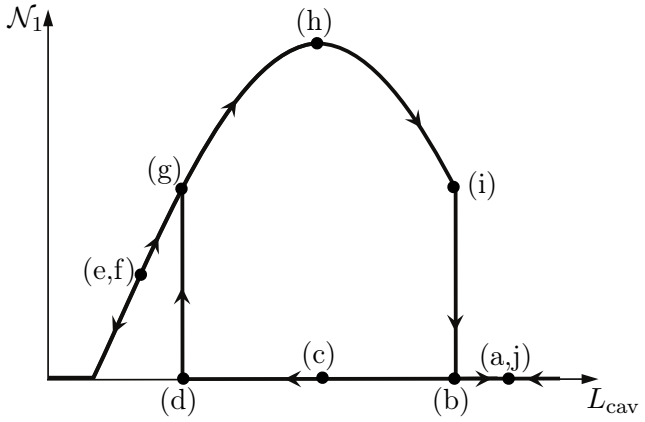

Figure 4.17: Evolution of the number of photons in mode 1 as a function of the cavity length, exhibiting a hysteresis cycle. Mode 2 exhibits the complementary evolution. The labels correspond to the subfigures of Figure 4.16.

The resulting evolution of the power of mode 1 as a function of the cavity length is thus summarized in Figure 4.17: depending on the direction in which the cavity length is scanned, $\mathcal{N}_1$ exhibits a different evolution, leading to the appearance of a *hysteresis cycle*. $\mathcal{N}_2$ exhibits the complementary evolution.

Figures 4.16 and 4.17 raise an interesting question. What happens if we start from the situation of Figures 4.16(c) and 4.16(h), where the two modes have the same gain and losses, and switch off the laser before switching it on again. When we switch on the laser, both modes have equal probability to end up oscillating in steady-state regime, but cannot oscillate simultaneously. And since the laser oscillation starts from nothing, there is no memory to "tell" the laser which mode it should choose. The answer to this question is that the laser actually does not start from nothing. It starts from spontaneous emission, which is intrinsically random. This means that the mode

that eventually wins is the one that first receives a spontaneously emitted photon. Switching on this laser is just like throwing a coin. This is another example of spontaneous symmetry breaking. But, contrary to Section 4.2.2b, the symmetry breaking occurs this time for a discrete variable that can take only two values (mode 1 or 2), and not for a continuous variable (the single-mode phase).

d. Role of the coupling constant on the laser behaviour

Beyond the case already mentioned above of an active medium exhibiting some inhomogeneous broadening, there are many situations in which two modes can oscillate, and where the mode competition that we have just discussed governs the behaviour of the laser:

- In the case of a bidirectional ring cavity, the two counter propagating modes compete for the gain. Depending on the spectroscopic details of the active medium, these two modes can oscillate simultaneously or exhibit bistabillity.
- In the case of a linear cavity, the laser modes are no longer traveling waves, but become standing waves, as shown in Figure 3.11. The presence of the spatial holes burnt by these standing waves in the population inversion leads to a decrease of the competition between the modes (see Figure 3.12).
- In the case of an inhomogeneously broadened active medium, depending on their frequency difference, two modes interact more or less with the same atoms. The strength of their competition will thus depend on their frequency difference (see Figure 3.7).
- Let us imagine a laser cavity that can sustain the oscillation of two orthogonally polarized modes, for example two orthogonal linear polarizations. Then, depending on the spectroscopic details of the active atoms or ions, the two modes may share the same amplifying atoms or not. Then the competition between the two modes can be more or less severe.

It is beyond the scope of the present chapter to address all these different situations. However, all these situations are governed by equations relatively close to the ones we have used in the present section. And, in all these cases, the key parameter is the coupling constant C. Indeed, the comparison between the situations of Figures 4.14 and 4.15 shows that the stability of the bistability solution and the simultaneity solution is governed by the order in which lines (β) and (δ) cross. We have seen in the preceding paragraphs that this depends on the value of the coupling constant C: when $C \leq 1$ the two modes may oscillate simultaneously, while when $C > 1$ only bistable

operation is possible. This constant C, which gives the ratio of cross- to self-saturation terms, consequently plays a central role in the dual-mode laser physics. And an important field of laser physics consists in adjusting the value of C to achieve the desired behavior for the laser.

This discussion can be generalized to a larger number of modes, but at the expense of a much more complicated formalism. For example, in the case of three modes, Figures 4.13, 4.14, and 4.15 must be replaces by 3D plots where on studies the intersection of planes.

Comment

The preceding discussion of the stability of solutions has been performed in the case of a class-A laser, allowing us to adiabatically eliminate the populations. One can show that the same conclusions, concerning the stability of the steady-state solutions, hold when one considers the full set of Equations (4.113–4.116). However, the transient behaviour of the laser depends on its dynamical class, as will be shown in Chapter 5.

4.5 Conclusion

This chapter has allowed us to derive the single-mode laser equations of evolution from the rate equation model that we developed in Chapter 2. We end up with two coupled nonlinear differential equations that describe the evolution of the two energy reservoirs that constitute a laser: the intracavity electromagnetic energy and the energy stored in the active medium in the form of atomic population inversion. The study of the steady-state solutions of these two equations have shown that the laser is a good illustration of some interesting features of nonlinear dynamical systems. Indeed, the steady-state laser has in general two steady-state solutions, the stability of which determines which one will be experimentally observed. By tuning a control parameter, such as the pumping rate, one can observe bifurcations, where one solution becomes unstable while the unstable one becomes stable. In the case of two modes, this physics becomes richer, since we now have several types of steady-state solutions, in which only one mode or two modes can oscillate. Furthermore, the competition between the two modes for the gain determines whether simultaneous oscillation is possible or not. In particular, in the case of strong competition, we have seen that the laser can exhibit bistability: an intriguing situation where two stable solutions exist, and the laser "chooses" between these two solutions based on its preceding history.

All these remarkable features are associated with the nonlinearity of the laser equations, due to the fact that the gain is a nonlinear function of the laser intensity, because of saturation. Thanks to this nonlinearity, the laser is close to many dynamical systems, such as for example the predator-prey situations governed by Volterra equations. In the following chapter, we will

see that similarly to these systems, the nonlinearity of the laser has even more interesting consequences when one studies its transient and dynamical behaviours and its fluctuations.